ISTANBUL TECHNICAL UNIVERSITY ★ GRADUATE SCHOOL

SYNTHESIS AND CHARACTERIZATION OF CARBON QUANTUM DOTS BY MICROWAVE HEATING METHOD

M.Sc. THESIS

Anita NABII

Department of Nano Science and Nano Technology

Nano Science and Nano Technology Programme

JUNE 2023

ISTANBUL TECHNICAL UNIVERSITY ★ GRADUATE SCHOOL

SYNTHESIS AND CHARACTERIZATION OF CARBON QUANTUM DOTS BY MICROWAVE HEATING METHOD

M.Sc. THESIS

Anita NABII
(513201004)

Department of Nano Science and Nano Technology

Nano Science and Nano Technology Programme

Thesis Advisor: Prof. Dr. Hilmi ÜNLÜ
Thesis Co-Advisor: Assoc. Prof. Dr. Seden BEYHAN

JUNE 2023

İSTANBUL TEKNİK ÜNİVERSİTESİ ★ LİSANSÜSTÜ EĞİTİM ENSTİTÜSÜ

MİKRODALGA ISITMA YÖNTEMİYLE KARBON KUANTUM NOKTALARININ SENTEZİ VE KARAKTERİZASYONU

YÜKSEK LİSANS TEZİ

Anita NABII
(513201004)

Nanobilim ve Nanomühendislik Anabilim Dalı

Nanobilim ve Nanomühendislik Programı

Tez Danışmanı :Prof. Dr. Hilmi ÜNLÜ
Tez Eş Danışmanı: Doç. Dr. Seden BEYHAN

HAZİRAN 2023

Anita NABII, a M.Sc. student of ITU Graduate School student ID 513201004, successfully defended the thesis/dissertation entitled "SYNTHESIS AND CHARACTERIZATION OF CARBON QUANTUM DOTS BY MICROWAVE HEATING METHOD", which she prepared after fulfilling the requirements specified in the associated legislations, before the jury whose signatures are below.

Thesis Advisor :	**Prof. Dr. Hilmi ÜNLÜ** Istanbul Technical University	.....
Co-Advisor :	**Assoc. Prof. Dr. Seden BEYHAN** Istanbul Technical University	.....
Jury Members :	**Prof. Dr. Mehmet Hikmet YÜKSELİCİ** Yildiz Technical University	.....
	Prof. Dr. Cevat SARIOĞLU Marmara University	.....
	Assoc. Prof. Dr. Caner ÜNLÜ Istanbul Technical University	.....

Date of Submission : 22 May 2023
Date of Defense : 08 June 2023

Dedicated to my spouse and Family…

FOREWORD

This thesis is written as a completion of my master's degree in Nanoscience and Nano-engineering program in the Physic and Chemistry Departments at Istanbul Technical University.

I would like to express my deepest gratitude and thank my supervisors, Prof. Dr. Hilmi ÜNLÜ, and Assoc. Prof. Dr. Seden BEYHAN for their guidance, understanding, and support along the way, but words cannot express my feeling enough.

Also, I would like to thank Dr. Mesut BALABAN for the support and helpful guidance that he has given me in relation to my research.

I would like to thank my friends especially Ramazan Ferhat ERDEN who helped me in doing laboratory work.

I must thank BİLİMSEL ARAŞTİRMA PROJELERI KOORDİNASYON BİRİMİ for supporting our project in terms of finances.

I thank Marmara University for X-ray Diffraction measurements, Tübitak for High-Resolution Transmission Electron Microscopy measurements, and Istanbul Technical University for Fourier Transform Infrared measurements of my samples.

I am very grateful to my parents and my sister for their infinite love, belief, and support who always motivate me throughout my academic journey and hardships. Also, they are always behind me and support me to make everything possible and smooth for me.

Finally, I am grateful to my husband, Amin for his support and consent to immigrate to Turkey with me due to my academic career, and I appreciate him owing to tolerating the difficulties along the way.

May 2023

Anita NABII
(Medical Engineering- Bio-electrics)

TABLE OF CONTENTS

Page

ABBREVIATIONS

A : Acetone
ABS : Absorbance
AN : Acetonitrile
C : Chloroform
CDs : Carbon Dots
CNTs : Carbon Nano Tubes
CNPs : Carbon Nano Particles
CQDs : Carbon Quantum Dots
E : Ethanol
EM : Emission
EX : Excitation
FTIR : Fourier Transform Infrared
FWHM : Full Width Half Maximum
GQDs : Graphene Quantum Dots
HRTEM : High Resolution Transmission Electron Microscopy
HT : Hydrothermal
J : Juice
M : Methanol
MW : Microwave
NH : N-hexane
NPs : Nano Particles
PL : Photoluminescence
QY : Quantum Yield
RFP : Regular Filter Procedur
TTDDA : Tridecanediamine
UV : Ultraviolent Visible Near Infrared
W : Water
XRD : X-ray Diffraction

SYMBOLS

A	**:** Absorbance
as	**:** Asymmetric
c	**:** Speed of light
d	**:** Distance Between the Atomic Layers
δ	**:** Bending
E (eV)	**:** Energy
h	**:** Planck's constant
I	**:** Integrated
n	**:** Integer
s	**:** Symmetric
η	**:** Solvent Refractive Index
θ	**:** Diffraction Angel
λ (nm)	**:** Wavelength
ν	**:** Frequency
ν	**:** Stretching

LIST OF TABLES

Page

LIST OF FIGURES

Page

SYNTHESIS AND CHARACTERIZATION OF CARBON QUANTUM DOTS BY MICROWAVE HEATING METHOD

SUMMARY

Carbon quantum dots (CQDs) have received considerable attention from researchers in recent years due to their rich features such as optical properties, abundance of functional groups on the surface, high solubility in water, low toxicity, and biocompatibility. In addition, they have applications in various fields such as bio-imaging, drug delivery, and photo-catalysis and they are low-cost and environmentally friendly.

In this thesis, carbon dots (CDs) were prepared by using orange juice as a carbon source and thiourea as a doping of nitrogen (N) and sulfur (S) with the microwave-assisted synthesis method, which is a low-cost and extremely useful method. The effect of adding the amount of thiourea was examined. Moreover, CQDs obtained by using citric acid instead of orange juice were compared. Synthesized carbon dots are analyzed by optical spectroscopy techniques (UV-Vis Absorption Spectroscopy, Photoluminescence (PL) Emission Spectroscopy), structural properties (X-Ray Diffraction (XRD), Transition Electron Microscope (TEM)) and in-situ Fourier Transform Infrared Spectroscopy (FTIR). According to the XRD result, the diffraction peak belonging to the carbon (002) is dominant and the interlayer distance value calculated based on this peak is approximately 0.32 nm, which is smaller than the graphite carbon. By analysis of TEM images, the particle size was determined to be in the range of 30-50 nm. The results obtained from the FTIR spectra show that N and S-doped CQDs contain various functional groups such as C=C, C=O, C-O-C -CS, -CH, C≡N, -NH, and –OH. The fluorescence quantum yield (QY) of CQDs obtained from orange juice, which was doped with thiourea was calculated according to the quinine sulfate standard. It was observed that the QY values increased by the increase of the amount of thiourea. However, there are limited studies on microwave-assisted synthesis methods, so we preferred to synthesize CQDs by this method, and the value of the highest QY was found approximately 7.1%. Photoluminescence (PL) emission properties depending on the excitation wavelength were examined in different solvent environments such as polar protic (water, methanol, ethanol), aprotic (acetonitrile, acetone), and non-polar (chloroform, n-hexane) in order to consider the effect of solvent polarities. We observed the emission wavelength due to excitation in all solvents towards red-shifted and these shift values changed according to the polarity of the solvents used. However, the PL emission intensity decreases with increasing solvent polarity when the excitation wavelength is greater than 325 nm. On the other hand, the observed PL emission intensity increased with the active role of functional groups in the core of CDs at excitation wavelengths lower than 325 nm excitation.

MİKRODALGA ISITMA YÖNTEMİYLE KARBON KUANTUM NOKTALARININ SENTEZİ VE KARAKTERİZASYONU

ÖZET

Karbon kuantum noktaları (CQDs), son yıllarda araştırmacılar tarafından giderek daha fazla ilgi görmektedir. Bunun sebepleri, optik özellikleri, yüzeydeki fonksiyonel gruplarının bolluğu, sudaki yüksek çözünürlüğü, düşük toksisitesi ve biyo uyumluluğu gibi zengin özelliklerdir. Ayrıca, bu noktalar düşük maliyetli ve çevre dostu olması nedeniyle nano sensör, biyo görüntüleme, ilaç salınımı ve foto kataliz gibi alanlarda da önemli potansiyele sahiptir.

Nano malzemeler ve kuantum noktalarıyla ilgili endişeler, düşük toksisite ve biyo uyumluluğudur, bu da karbpn noktalarının özel özellikleridir.

Ayrıca, bu noktalar düşük maliyetli ve çevre dostu yöntemlerle sentezlenebilir. Bu yöntemler, sitrik asit , portakal suyu, pirinç ve kahve çekirdekleri gibi heterojen kaynakları içermektedir.

CQD'ler nano sensör, biyo görüntüleme, ilaç salınımı ve foto kataliz gibi alanlarda da önemli potansiyele sahiptir. Buna ilaveten, karbon kuantum noktalarının yapısı genellikle amorf bir karbon yapıdan oluşur ve kenarlarında oksijen ve azot gibi bazı kusurlar bulunmaktadır.

Bu tezde CQD' ler, ucuz ve son derecede kullanışlı bir yöntem olan mikrodalga destekli sentezle hazırlanmıştır. karbon kaynağı olarak portakal suyu tercih edilmiş ve azot (N) ve sülfür (S) katkısı olarak tiyoüre kullanılmıştır. Ayrıca, İlave edilen tiyoüre miktarının CQD'lerın özellikleri üzerindeki etkisi de incelenmiştir. Aynı zamanda portakal suyu yerine sitrik asit kullanılarak elde edilen CQD' lar karşılaştırılmıştır.

Filtrelemenin sentezleme üzerindeki etkisini bilmemize bağlı olarak, iki farklı yöntem kullandık. Filtreleme yöntemlerimiz, kromatografi sütunu ve Standart Filter Prosedür (RFP) filtresi olarak adlandırdığmız bir yöntemdir. RFP filtre vakum, şırınga ve santrifüj yöntemler içermektedir. Portakal suyu ve 2 g tiyoüre ile CQD'ler sentezledik ve bu filtereleme yöntemlerini kullandık. Ayrıca, bu iki örneği X-Işını Kırınım (XRD) ile analiz ettik.

Portakal suyu ve 0.3 g, 1.5 g ve 2 g tiyoüre ile elde edilen CQD'ler örneği, uyarlama dalga boyu olarak 325 nm ve 350 nm'de farklı fotolüminesans yoğunluklarına sahip oldukları için seçildiler. Ayrıca, sitrik asit ile elde edilen CQD'lerin tiyoüre miktarı aynıdır.

3D kontur haritasından açıkça görülebilmektedir ki, portakal suyunda tiyoüre katkısının ve sitrik asidin fotolüminesans (PL) emisyon şiddetinın üzerindeki etkileri birbirine zıttır. Sitrik asitte tiyoüre katkısının etkisi sonucuna göre, fotolüminesans emisyon şiddeti tiyoüre katkını artışıyla tamamen bastırılmıştır, muhtemelen yüzeyde su ile hidrojen bağı oluşmasından kaylanmaktadır. Maksimum emisyon dalga boyu, 450 nm' den 430 m'ye kadar değişim gösterir. Bu kontur haritasına göre, sitrik asit ve 0.3 g tiyoüre ile elde edilen CQD'lerde üç farklı bileşen bulunmaktadır. İlk bileşende,

350 nm'de uyarladığında kırmızı bölgede maksimum 450 nm 'lik bir emisyonla birlikte emisyon artışı görülür. İkinci bileşen ise mavi bölgededir ve 270 nm'de uyarılığında 480 nm'de pik yapar. Üçüncü bileşen ise, 430 nm'de uyarıldığında PL emisyon dalga boyu 520 nm'ye kayar.

Bunun aksine, tiyoüre katkının artışıyla portakal suyunda PL emisyon şiddeti artar. Uyarlama dalga boyunun ve tiyoüre miktarının (0.3 , 1.5 , 2 g) PL emisyon yoğunluğu üzerindeki etkisi, 330 nm'de uyarladığında kırmızı bölgede maksimum değere (400 nm) sahip bir artş gösterir. Ayrıca, her iki nemune uyarlama dalga boyuna bağlıdır.

Sentezlenen CQD' lerın optik spektroskopi teknikleri (UV-Vis Absorpsiyon Spektroskopisi, Fotolüminesans (PL) Emisyon Spektroskopisi), yapısal özellikleri (X-Işını Kırınım (XRD), Geçirimli Elektron Mikroskop (TEM)) ve in-situ Fourier Dönüşümlü Infrared (FTIR) Spektroskopi gibi çeşitli analiz teknikleri kullanılarak incelenmiştir.

XRD sonucuna göre, analiz edilen nemunelerde karbon (002) düzlemine ait kırınım piki baskındır ve bu pike bağlı olarak hesaplanan düzlemler arası uzaklık değeri yaklaşık 0.32 (RFP filtresi ile filterlenen örnek) nm ve 0.36 (kromatografi sütunu ile filterlenen örnek) belirlenmiştir. Bu değerler, grafit karbondan daha küçük ve büyük bir uzaklık değerini ifade etmektedir. 0.36 nm, grafitik ara tabaka aralığından daha büyüktür ve CQD'lerin doğası zayıf kristal yapıya sahip olduğunu göstermektedir. Bu nedenle, RFP yöntemiyle elde edilen sonuçlar kafes parametrelerine göre daha makul görünmektedir.

TEM görüntülerinin detaylı analizi ile, parçacık boyutlarının 30-50 nm aralığında olduğu tespit edilmiştir. Ancak, sonuç olarak, TEM görüntüleri elde edilen CQD'lerin yapısındaki 'd' aralıkları, çizgi oluşumları veya kusurlar gibi ek özellıklerin gözlemlemesi mümkün değildir. Bunun muhtemelen çözünürlük ve görüntü faz kontrasıyla ilgili olduğu düşünülmektedir.

FTIR spektrumlarından elde edilen sonuçlara göre, N ve S katkılı CQD' lerinin çeşitli fonksiyonel grupları içerdiğini göstermektedir. Bu gruplar arasında C=C, C=O, C-O-C -CS, -CH, C≡N, -NH, ve –OH gibi çeşitli bağlantılar bulunmaktadır.

Ayrıca, tiyoüre ile katkılanan ve portakal suyundan elde edilen CQD' ların floresans kuantum verimi (QY), kinin sülfata standardına göre hesaplanmıştır.Bu hesaplama, CQD'ların floresans özelliklerini değerlendirmek için kullanılan yöntemdir. Floresans kuantum verimi, CQD'ların ne kadar etkili bir şekilde ışığı emip ve yeniden yaydığını gösterir.

Bu sonuçlar, CQD'ların floresan özelliklerinin belirlenmesi ve potansiyel uygulamalarında değerlendirilmesi için önemli bi bilgi sağlamaktadır. Analizlere göre, thiyoüre miktarının artmasıyla parçacık boyutu küçülür, bu nedenle parçacık boyutu azaldıkça QY değerinin arttığı söylenebilir. Bu sebeple, Katkı miktarının artışıyla birlikte QY değerlerinin arttığı gözlemlenmiştir. Bu durum, CQD'lerin optik özelliklerinin katkı miktarına bağlı olarak iyileştiğini göstermektedir. Bununla birlikte, mikrodalga destekli sentez yöntemleri ile ilgili sınırlı sayıda çalışma olduğundan, bu yöntemi CQD'leri sentezinde tercih ettik. Yapılan çalışmalar sonucunda, mikrodalga destekli sentez yöntemiyle elde edilen CQD'lerin en yüksek kuantum veriminin değeri yaklaşık %7.1 olarak bulunmuştur.

CQD'ler, karboksil, hidroksil ve karbonil gruplarının varlığı sayesinde protik ve aprotik çözücülerde kolaylıkla dağlabilir. Fakat, karbon noktaları apolar çözücülerde

dağılamazlar. Ek olarak, karbon noktaları ile çözücüler arasındaki etkileşim, PL emisyon dalga boyunda hayati bir rol oynamaktadır.

Solvent polaritelerinin etkisini incelemek amacıyla, farklı çözücü ortamlarında (polar protik, aprotik ve apolar), uyarılma dalga boyuna bağlı photoluminescence (PL) emisyon özellikleri incelenmiştir. Bu çalışmada, solvent polaritesinin karbon kuantum noktalarının floresans özellikleri üzerindeki etkisini belirlemek için sırasıyla (su, mthanol, ethanol, asetonitril, aseton, kloroform, n-hekzan) gibi çeşitli solventler kullanılmıştır.

Yapılan analizlere göre, tüm çözücüler de uyarılma dalga boyuna bağlı olarak emisyonun kırmızıya doğru kaydığı gözlemlenmiştir. Ancak, bu kayma değerlerinin kullanılan çözücülerin polaritelerine bağlı olarak değiştiği belirlenmiştir. Bununla birlikte, PL emisyon incelendiğinde, çözücü polaritesinin artışıyla birlikte uyarılma dalga boyunun 325 nm' den daha büyük olduğu durumlarda PL emıisyon azaldığı gözlenmiştir. Buna karşı, 325 nm' den daha düşük bir uyarılma dalga boyuna sahip CD' lerin çekirdeğinde yer alan fonksiyonel grupların etkin rolü gözlenmiştir. Bu gruplar, PL emisyon şiddetini artırabilir.

1. INTRODUCTION

Carbon dots (CD, C-dots, and CQDs), an appearing category inside the carbonaceous groups, are small particles that are sized less than 20 nm [1]. CDs structure includes a carbon core, usually amorphous with a crystalline domain [2]. In addition, there are some defects in its edge that heteroatoms like oxygen and nitrogen atoms introduce, and different functional groups or fluorescent molecules connected to the core surface [2]. They have obtained a variety of notices owing to their optical properties, plentiful surface chemistry, water solubility, low toxicity, and biocompatibility since they were discovered during purgation preparative electrophoresis of single-walled carbon nanotubes conducted in 2004 [3,4,5,6]. The interest in this discovery is elaborated because they can be synthesized from cheap and eco-friendly methods that consist of citric acid and heterogeneous sources that include orange juice, rice, and coffee beans [7]. Furthermore, the principal biological properties of C-dots, such as biocompatibility and low toxicity lead to accomplished potential applications in bio-sensing, bio-imaging, photo-catalysis, and drug delivery [6], and the major concerns about nanomaterials and quantum dots are low toxicity and biocompatibility which are the special characteristics of CDs [8]. CDs are synthesized by top-down or bottom-up methods. The top-down synthesis starts from bulk carbon precursors that are cut down to nanosized dimensions using physical and chemical methods, such as Laser Ablation, Electrochemical method, and Arc Discharge, Ultrasonication [3,9]. In contrast, the bottom-up synthesis starts from a mix of small organic molecules that goes through pyrolysis. Through polymerization, the carbonization of the precursors can be achieved by Microwave, Hydrothermal, or Thermal treatments [9].

The characterization methods of C-dots are Ultraviolent Visible Near Infrared (UV – Vis-NIR) Spectroscopy, Photoluminescence (PL) Spectroscopy, X-ray diffraction (XRD), High-resolution Transmission (HRTEM), Fourier Transform Infrared Spectroscopy (FTIR) and Raman Spectroscopy. In addition, CQDs include high-oxygen contents and it is known as “carbogenic nanodots” [10]. The amount of oxygen in CDs is in the range of 10%- 50%. Also, it can be in functional groups on

the surface, and it can cause low quantum yield (QY) since the bare surface of CDs is exposed so it can be harmed. QY measures the capability of a particle to emit the absorbed energy of photons [10].

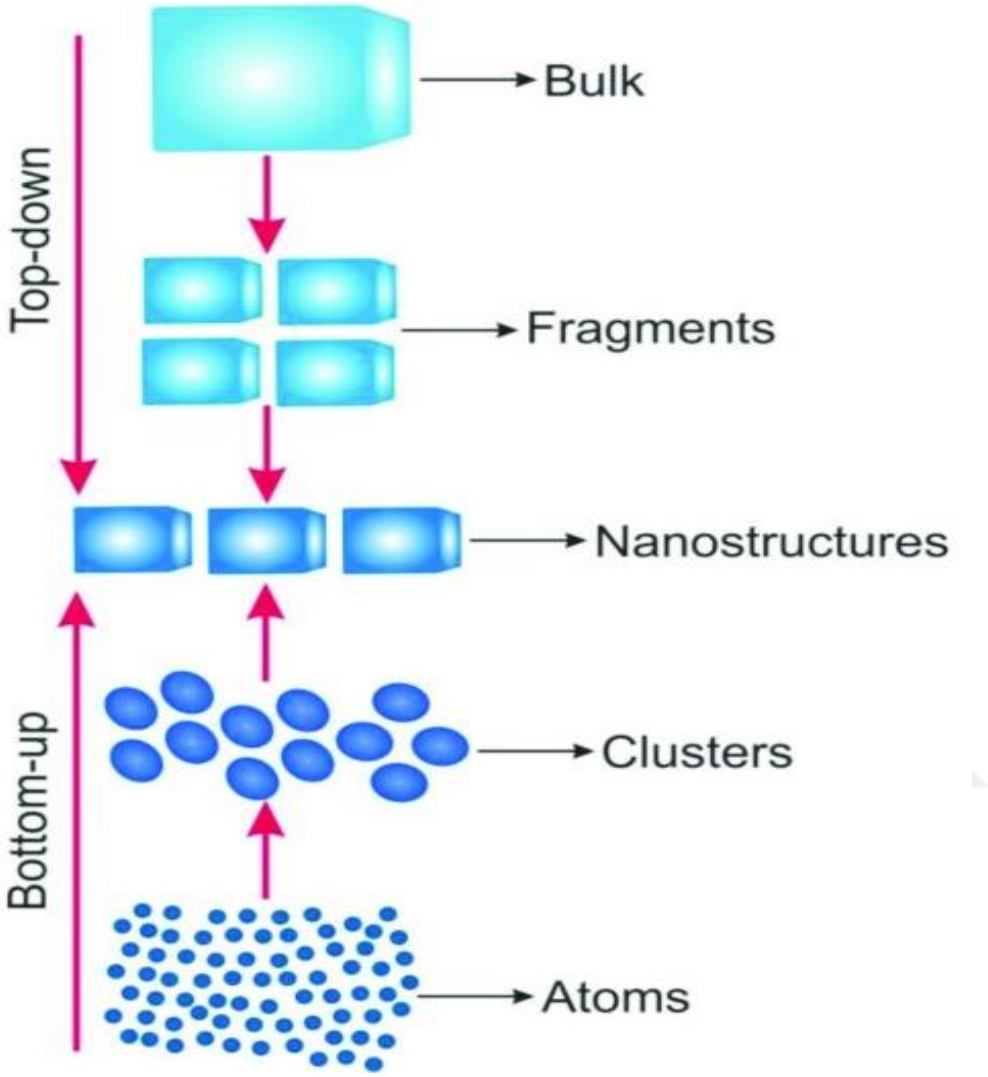

Figure 1.1 : Schematic of top-down and bottom-up approaches [11].

The surface passivation layer is one of the methods to increase the QY, for more explanation, this method protects the surfaces of the CQDs. This raised stability results in higher QY and long-term use [10]. Surface passivation is concluded by polymeric chains like polyethylene glycol attached to the surface of CDs to build a thin barrier layer that supported CDs from impurity adherence and enhances PL intensity [10]. N-doped CQDs improved QY, in this method, some of the carbon atoms are replaced by nitrogen atoms in the core structure or N-containing groups at the edges [10]. The highest amount of QY for N-doped CDs is 93.3% from citric acid and tris aminomethane [10]. Citric acid and urea are inexpensive precursors for CQD

synthesis. Citric acid has four active groups three COOH and one OH and urea has two amine groups that give water-solubility properties [10]. Doping elements such as Sulfur and Nitrogen can be used to adjust the optical properties of carbon dots (CDs) in terms of emission and excitation wavelengths, as well as fluorescence intensity. The effect of doping elements on CDs is attributed to the alteration of orbital energy levels between the lowest unoccupied molecular orbital (LUMO) and the highest occupied molecular orbital (HOMO) [12].

One of the most important properties of CDs is their accessibility in nature. Because of that, orange juice can be used for producing CDs since it is one of the best natural resources. Orange juice is composed of organic acids, sugars, and phenolic compounds. The principal organic acids discovered in orange juice are citric, malic, and ascorbic acid [13]. The citric acid in orange juice is a carbon source for synthesizing c-dots. Additionally, thiourea is an organosulfur compound with the formula $SC(NH_2)_2$. Its structure is similar to urea, but the sulfur atom is replaced by the oxygen atom of urea. In addition, thiourea is an element of doping precursor. It can dop S and N. The content of N and S dopes can enhance the fluorescence intensity, and increase the QY and emission behavior of C-dots [10, 14]. The microwaving heating way which is one of the bottom-up approaches, and this technique holds significant promise in the field of green chemistry, providing a flexible platform for the formation of heterocycle rings [15]. Additionally, the Mw synthesis method is more convertible, speedier, and more homogeneous in heating carbon precursors than other methods [15]. Microwave irradiation has an insight characteristic, which makes it possible to homogeneously heat the reaction solution [15]. This method is also simple, safe, and environmentally friendly [15].

1.1 Synthesizing Methods

The laser ablation method involves using a high-intensity laser beam to eliminate material from the surface [6, 9]. Laser ablation is a common method for synthesizing carbon nanomaterials [9]. In 2006, Sun and co-workers used this method for synthesizing C-dots by baking graphite with cement [6, 16]. After surface passivation with poly (ethylene glycol) and poly (propionyl ethyleneimine-co-ethyleneimine), only the nanoparticles could become CDs. Carbon suspensions in different solvents, which can passivate directly the carbon nanoparticles were used in this method for

synthesizing more CDs, but complicated preparation procedures could limit the development of CDs [6].

The arc discharge method is used to produce carbon nanotubes. In this method, small graphitic electrodes with a diameter of 1 mm or less are subjected to high electrical currents under an inert gas atmosphere, typically argon or helium [9, 17]. The vaporization of carbon generates carbon nanoparticles, which are sediment on the cathode. In addition, this method not only is simple but also purifies carbon dots from the heterogeneous mixture of carbon nanoparticles with low yield [9].

The electrochemical method involves the generation of carbon nanodots by either forming or peeling off from a large carbon structure [18]. In this method, there are kinds of conductive carbonaceous materials (carbon fiber, graphite rod, etc.) [18]. In an electrolyte solution, a carbon anode and a cathode could be applied electrical potential then the graphitic carbon source exfoliates to form, as proved by Lu et al [9]. Oxidative cleavage of carbon anode connected with intercalation of ions is a common mechanism of graphite quantum dots (GQD) generation [9].

The ultrasonic treatment is another method of the top-down approach. In this method, the large carbon materials can be collapsed by the action of extremely high energy of ultrasonic sound wave [3]. Li et al. indicated that CNPs could be synthesized by ultrasonic method for activating carbon dispersed in a hydrogen peroxide solution [9]. In addition, Wang et al. synthesized N-doped carbon dots with ascorbic acid and ammonia via ultrasonic treatment [3].

Pyrolysis is an extremely efficient process and valuable technique used to collapse large graphitic carbon structures into smaller ones, including CNTs, fullerenes, and nanodiamonds. This process involves subjecting carbon precursors to high temperatures under acidic or basic conditions, resulting in the formation of smaller carbon structures known as CDs while simultaneously passivating them [9]. Moreover, owing to the high energy generating of pyrolysis it triggers the formation of reactive species that have the capability to bond with other molecules during the carbonization process. This enables the production of carbon nanomaterials using smaller carbon sources like organic molecules and polymers. Therefore, C-dots are commonly made by pyrolysis from various carbon sources [9]. The main and important advantage of this method rather than top-down approaches is its ability to use a variety of carbon

precursors, however, top-down approaches commonly use graphitic carbon materials as precursors [9].

The hydrothermal method is one of the common synthesizing methods of carbon nanostructure of the bottom-up approach category. The main point of this method is the solubility of minerals in hot water under high pressure which single crystals depend on it during synthesizing [19]. In this method, biomass, and organic waste in the presence of water change to solid biofuel, liquid, and gaseous products [19]. For this transformation of waste of different origins, low energy is needed. In addition, some parameters are crucial for the properties of the result of the products such as residence time of reaction, pH, water content, and temperature. Moreover, accurate adjustment is highly crucial and has a considerable shock on the properties of hydrothermal products [3]. Zhang et al. synthesized fluorescent Carbon dots from a small organic compound, l-ascorbic acid via the hydrothermal method for the first time. The aqueous solution of ascorbic acid was heated at a steady 180 °C temperature for durations of 4h in an autoclave. Subsequently, the water-phase solution was purified through dialysis [3]. Li et al. constructed water-soluble Nitrogen-doped CDs by using ammonium citrate and ethylenediamine. The aqueous solution of ammonium citrate and ethylenediamine was heated at a steady 200 °C temperature for 5h. The quantum yield was found (QY) 66.8% [3].

The microwave‑assisted synthesis method is extremely convenient, very fast, and low-cost to synthesize CDs. In addition, this method is more homogeneous heating of carbon precursors than other methods [3]. Microwave allows heating happens in a shorter time, also, commercial microwave oven works in this period [3]. Guan et al. explored this method for the development of luminescent C-dots with folic acid molecules as both nitrogen and carbon sources [6]. At first, the 15 g folic acid was blended in 3 mL diethylene glycol, and this solution was placed in a domestic microwave at 750 W for 40 min. The color of the suspension, which was obtained, was red-brown, and its dialysis was carried out for 3 days against pure water [6]. Also, Zhu et al. synthesized fluorescent carbon dots via the microwave heating method for the first time. An aqueous solution of saccharides and polyethylene glycol was heated by a domestic microwave oven at 500 W for 3 min [20]. Moreover, Liu et al conducted a synthesis of multicolor photoluminescence carbon dots by utilizing glycerol as the carbon source 4, 7, 10-trioxa-1,13-tridecanediamine (TTDDA) as the passivating

agent [21]. Wang et al. synthesized water-soluble carbon dots via microwave heating pyrolysis of citric acid. Tryptophan served as both a passivating agent and nitrogen source in the experiment. The solution containing citrate and L-Trp was heated in a microwave at 700 W for 3 min, and the large particles were eliminated by centrifuging at 10,000 rpm [21]. Citric acid was used as a carbon source and 3-aminophenyl boronic acid as the passivation agent to make CDs by Kiran et al. They heated the solution of citric acid and 3-aminophenyl boronic acid in a microwave oven at 1200 W for 4 min [21].

1.1.1 Synthesizing S-doped and N-doped carbon dots

Nitrogen and Sulfur can dop carbon dots with high fluorescence quantum yields (FLQY= 25%) via the microwave-assisted method. Concurrent doping of N and S effectively enhanced electron transfer and coordination interaction between N, S/C-dots, and Hg^2 [22].

Sulfur-doped carbon dots were synthesized by using a microwave-assisted method with succinic acid and sodium thiosulfate as the precursor materials. Succinic acid and sodium thiosulfate were chosen as they were biocompatible and contained carbon and oxygen elements. Succinic acid forms a carboxylic functionalize group [23]. The findings of their study revealed that the synthesized S-CDs exhibited a spherical morphology and were dispersed within the size range of 1.5-5.0 nm [23]. The XRD spectra showed the degree of crystallinity of the S-CDs synthesized indicated sharp peaks around 25.47°–28.06° [23]. The optical properties of S-CDs were analyzed by UV–Vis and fluorescence techniques. There were two unique absorption peaks. The peak at 255 nm corresponds $\pi \rightarrow \pi^*$ transition of C=C and the peak at 320nm corresponds to $n \rightarrow \pi^*$ transition of C=O [23].

Synthesis of N-doped carbon dots via a hydrothermal technique using tangerine juice, onion shell, and ethylenediamine [24]. Peaks were at 285 nm and 347 nm in the UV-vis spectrum, and they proved the C=O and C=N bonds. It could show that there was a redshift in the absorption peak owing to the amine groups in the structure of the N-doped carbon dots. The XRD pattern indicated that the N-doped carbon dots exhibited an amorphous structure [24].

1.2 Characterization Methods

Size and shape are two main parameters of the characterization of NPs. In addition, the size distribution, degree of aggregation, surface charge, and surface area, and to some extent evaluate the surface chemistry can be measured. There are widely used methods for characterizing carbon quantum dots that are mentioned.

UV-Vis-NIR Spectroscopy is the method to discover the optical properties of liquids and solids [9]. It can measure how much a chemical substance absorbs light [9]. This device shows the peak of absorption. Therefore, the C-dots are synthesized by different techniques analyzed by this device for known strong UV absorption of them; however, the positions of absorption peaks vary depending on the specific synthesis methods employed [6]. The accurate spectral position depends on different factors such as size, type, and extent of carbon bonds (sp^2 vs sp^3), solvent, and passivation [9].

GQD and CQD with more sp^2 carbon the maximum absorbance peaks are around 250-300 nm via $\pi \rightarrow \pi*$ transition, but the maximum peak can occur at longer wavelengths that are dependent largely on the surface passivation [9]. In addition, carbonyl (C=O) or carbon-nitrogen (C-N) bonds have electrons at the n state level which has a higher energy level than the π state which has indicated the absorbance result at even higher wavelengths operator transitionation, from 350 nm to visible ranges, so other functional groups can cause π-electron delocalization of the sp^2 carbon system [9].

Li et al. used hydrogen peroxide and active carbon. They added 4 g of active carbon into 70 mL of hydrogen peroxide for preparing suspension and mixing for 2h at room temperature. After filtration, the absorption band peak of fluorescent CDs which were water-soluble was displayed at 250-300 nm [6].

Dong et al. obtained carbon dots by using carbonation of citrus acid at 200 °C. The absorption range is 362 nm [6]. Also, the narrow peak width showed that NPs sizes were consistent, and the maximum emission wavelength did not change when activated at the different excitation wavelengths [9]. Tang et al. used the microwave heating method for doing pyrolysis of a glucose solution assisted in making carbon dots; the QY of obtained CDs was 7-10%. There were two absorbance peaks at 228 and 282 nm were shown by the aqueous solution of these C-dots. When the power of heating of the microwave increased the intensity of the two peaks increased, too.

Although, the positions of the peak remained steady and indicated no connection with NPs size [6].

PL Spectroscopy is when light energy, or photons, prompts the emission of a photon from any stuff. Moreover, PL is the most appealing characterization of C-dots [9]. Photoluminescence has been used for optical characterization methods owing to its non-destructive nature and capability to yield important information about intrinsic and extrinsic transitions [25]. One of the most important and significant aspects of PL of carbon quantum dots is the excitation-dependence of emission intensity and wavelength [9]. For more illustration, an emission spectrum displayed the wavelengths of the spectrum that an energetic object emitted [9]. The excitation spectrum is scanned when the emission wavelength is fixed.

The size and shape of CDs display the influence of photoluminescent behavior. By increasing the size of the nanoscale, the energy bandgap decreases, so the emission happens at longer wavelengths (redshift) [9]. Kim et al. approved the influence of size-dependent properties on GQDs by changing their average size range. They found that when excited at 325 nm, the PL emission of GQDs exhibited a redshifts as the GQD size increased from 5 nm to 35 nm. Moreover, the peak of absorbance in the same size range happened at longer wavelengths, and the intensity reduced with growing GQD size [9].

X-ray diffraction (XRD) is a powerful nondestructive technique used for characterizing crystalline materials. It provides vital information about the structure, phase composition, crystal orientations, and other structural parameters like average grain size, crystallinity, strain, and crystal defects. It is widely employed for analyzing and understanding the properties and behavior of crystalline materials. XRD peaks are generated through the constructive interference of a monochromatic X-ray beam scattered at significant angles from different sets of lattice planes within a sample [6]. The peak intensities are shown by the division of atoms inside the lattice [26]. XRD is significantly used to characterize C-dots and to gain information on particle size, phase purity, and crystal structure [26]. Liu et al. synthesized C-dots with hexa-peri hexabenzocoronene as the precursor. CDs with a size of 2-3 nm thickness and approximately 60 nm in breadth were produced, after pyrolysis at high temperatures, surface functionalization decreases treatment, and oxidative peeling. Therefore, the C-dots gained possessed a fluorescence QY of 3.8% [6]. Through one-stage pyrolysis of

poly (acrylic acid), Mao et al. created photoluminescent C-dots with glycerol. The C-dots' varied structures and optical characteristics were all explored. The XRD displayed a wide peak of approximately $2\theta = 24°$, moreover confirming the graphite structure of the white luminous C-dots [6]. Bourlinos et al. synthesized CDs with the calcination of ammonium citrate salt at 300 °C; the related XRD graph displayed two reflections that were superimposed, which approved the presence of exceptional carbon alkyl groups that were surface altered [6].

The High-resolution TEM (HRTEM) is determined by the direct image of the atomic structure of samples [6]. The details about the crystallographic structure of materials from images and high-phase contrast images were obtained. This method is commonly used in the characterization of materials leading to the gained of details about punctual defects, stacking faults, precipitates, and grain boundaries [9]. In addition, the crystalline nature of C-dots is classified into two types of lattice fringes: interlayer spacing and in-plane lattice spacing. Interlayer spacing is around 0.34 nm, whiles in-plane lattice spacing is 0.24 nm. Zhang et al. synthesized C-dots with acid oxidation of graphite, in addition, their lattice spacing was less than 0.3 nm, showing that a large portion of C-dots was separate graphene. Shinde and Pillai synthesized C-dots from multi-walled carbon nanotube dots via the electrochemical method, and at the same time, two kinds of lattice fringes were observed in the high-resolution TEM image [6].

The Fourier Transform Infrared Spectroscopy (FTIR) method is employed for identifying functional groups present on the surface of carbon quantum dots. C-dots contain oxygen, carbon, and hydrogen C-dots are formed through the partial oxidation of a carbon precursor, resulting in an abundance of carboxyl or carboxylic acid groups, hydroxyl groups, and ether/epoxy on their surface. Therefore, FTIR is commonly used for the investigation of these groups including oxygen [6]. In addition, modifying carbon dots can be characterized by infrared spectroscopy to decide if they are passivated enough [6]. Peng et al. evolved C-dots with sizes ranging from 1 to 4 nm by oxidizing carbon strands measuring of one micron. These 1-4 nm C-dots exhibited solubility in a polar solvent, water; dimethyl sulfoxide, and dimethyl formamide [6]. The infrared peaks of characteristic absorption at 1724 cm^{-1} and 3307 cm^{-1} proposed carboxyl groups' display on their surface [6]. The presence of a double bond was indicated by the peak of absorption at 1579 cm^{-1}, and the presence of ether linkage was implicit by an absorption peak at 1097 cm^{-1} [6].

Raman Spectroscopy: This device is non-destructive, strong, and sensitive for characterizing carbon materials and nanostructures. Raman process is an inflexible light scattering process. The energy difference between the incoming and the scattered light meets the energy of the molecular vibrations or elementary excitations [27]. Phonons or charge density waves are examples of this matter [27]. Changes in the atomic bonds or molecular structures of probed samples can modify the Raman peaks, so the detail of structural order and the degree of graphitization of soot can be acquired [27]. Das et al., Yan et al., and strain Huang et al. showed in their studies there are two significant Raman bands D and G bands in the frequency range between 1000 and 2000 cm^{-1} in carbon-related materials, like carbon nanotubes and graphene. The D (for "Defect" or "Disorder") and the Raman band (centered at around 1350 cm^{-1}) is a disorder-induced bands. Its intensity and linewidth usually increase with the density of defects/impurities in the sample. The G (for "Graphite") Raman band, centered at about 1600 cm^{-1}, is also sensitive to sample quality. It emerges from the stretching of C-C bonds. In graphene layers, the frequency and linewidth of the G band are a symbol of charge carrier density [28].

2. EXPERIMENTAL

2.1 Materials

The materials and reagents used in this work contained: fresh orange juices purchased from local restaurants in Istanbul/Türkiye. Anhydrous citric acid (Tekkim, Türkiye). Thiourea (Sigma-Aldrich, USA), and distilled water (Hayat su, Türkiye) for the preparation of CDs. As solvents: methanol (Tekkim, Türkiye), ethanol (Merck, Germany), acetone (Tekkim, Türkiye), Chloroform (Merck, Germany), n-hexane (Merck, Germany), and acetonitrile (Merck, Germany). The materials for chromatography include sand (Tekkim/Türkiye), Silica gel (Tekkim, Türkiye), and Ethyl acetate (Merck/Germany). For quantum yield: Quinine Sulfate (Sigma-Aldrich, Germany) and H_2SO_4 (Merck, Germany). Rotofix 32A Centrifuge (Hettich, Germany), vacuum drying oven (Heraeus vacuum oven, Thermo Scientific, Born/ Germany), Ultrasonic cleaner (CD-4820, China), UV-VIS-NIR Spectrophotometer (UV-3600, Shimadzu, Japan), Cary Eclipse fluorescence spectrophotometer (California, USA), D2 PHASER Bruker XRD (China). HRTEM (Oxford Instruments X-Max 80-T EDS, Germany). FTIR spectrometer (Nicolet 6700, Thermo Scientific).

2.2 Method

2.2.1 Method of filtration

Filtration is a physical separation technique employed to separate solid particles from a mixture by passing it through a filter, thereby separating the solid matter from the fluid [29]. Filtration can make the solution pure and it has a crucial role in the experiments. In Figure 4.1 the importance of filtration is obvious. Therefore, selecting the way of filtration is more important. We used two methods of filtration and compared with together (Figure 4.2).

Two methods of filtration were used in this experiment. The first way is a vacuum filter, syringe, and centrifuge. In contrast, the second way is a chromatography column filter. Column chromatography is simple and the most popular separation and

purification technique. Column chromatography was made up of a stationary solid phase like silica gel that adsorbs and separates the C-dots passing through it with the help of a liquid mobile phase like ethyl acetate [30]. The Ethyl acetate plays an important role in the separation of C-dots [30]. It is used to separate C-dots, then each of these beakers was analyzed by UV, and PL spectroscopies. On the contrary, the regular filtration method like the vacuum with an air intake engine. Orange juice was vacuumed by this filter twice then we used a syringe filter and then we separated 20ml of this pure orange juice for adding thiourea. After burning the solution and stirring it we used a vacuum filter twice and a syringe filter again then we used a centrifuge for 15 minutes at 4000 rpm. In addition, a syringe filter was used after centrifuging, too. Therefore, we could obtain greater results with a regular filter. These results are for 10µl of each sample. In addition, the sample with 2 g thiourea with orange juice is filtered by these methods and analyzed by XRD (Figure 4.17). Figure 4.2 shows the role and importance of the filtration method in the experiment.

2.2.2 The synthesizing method

First, Fresh orange juices were filtered by a vacuum filter once. (In some experiments they were filtered by vacuum twice). Afterward, syringe filters were used for filtering. For sample preparations, 20 ml of pure orange juices was enough for our study. Moreover, certain amounts of thiourea (0.05 g until 2 g) were added to the sample. Then the sample was stirred at 600 rpm for 15 min. The solution was placed in the ultrasonic cleaner for 480 secs. Then it was placed in the microwave oven at 800 W. Next, it was placed to cool down for 8 mins. After cooling down, 50ml distilled water was added to the sample. Then the samples were stirred at 600 rpm for 15 minutes, 2:14 h. Next, the mixture was placed in the ultrasonic cleaner two times (480 secs). Afterward, the solution was filtered by a vacuum filter for varying times as well as filtered with syringe filters for a second time. After that, in some experiments, this solution was centrifuged for 15 minutes at 4000 rpm and they were filtered by syringe filters. Moreover, for noticing the actions and performances of some solvents (polar protic, polar aprotic, and non-polar) with certain samples, we measure the phentolamines spectroscopy in certain excitations wavelength. In addition, for samples with 2 g thiourea, after doing the vacuum filter once, the chromatography method was applied. Then the as-prepared solution is ready for measurements by UV Spectroscopy and PL Spectroscopy.

In the second experiment, we used citric acid, and thiourea.

In 1000 ml orange juice is 16 g citric acid, so in 20 ml orange juice has 0.32 g citric acid. Therefore, we stirred 0.32 g citric acid with 20 ml distilled water for 5 minutes, then used 0. 3, 1.5, and 2 g thiourea again. The procedure was similar to the previous experiments.

2.2.3 Characterization

UV-Vis-NIR Spectroscopy is one of the methods that we used for the characterization of our samples. This device has two cuvette holders that are for reference and sample. After opening the program, we pressed connect to make the connection between the device and the computer. In the method section, we set the wavelength to 200-600nm wavelength and we set the absorbance tab for measuring then we pressed baseline and auto zero. After this procedure, we placed references and samples in the holders.

PL Spectroscopy: We measured the PL of samples in different emission wavelengths and excitations. For PL measurements, 0.15 abs at 380 nm wavelength are chosen due to two reasons. The first reason is that in different numbers of excitations, the absorbance amount should be equal and the second reason is self-absorption. Self-absorption refers to the ratio of fluorescence signals measured by the incident and emitted ion chambers. This ratio is accurate only when the samples are very thin or much diluted [31]. To achieve this, we used the UV-Vis spectrophotometer. We used the option of Go To WL and type our considered wavelength (in our case, it was 380nm). After that, we placed the reference sample and sample into the two cuvettes. If its absorbance was higher than 0.15 a.u. we diluted more with the reference sample and if conversely, matter happened we added more of the sample to the cuvette. Therefore, the PL sample was prepared to measure in eight excitation wavelengths. In addition, we prepared our solvents and samples by adding a little amount of our sample in the solvents which are in the cuvette and made their absorbance at the same level then we measured their PL In seven excitation wavelengths. Our device is the Cary Eclipse fluorescence spectrophotometer (California, USA). In the PL program, the Scan program is needed. In the data mode, we set eight excitations (from 300 to 450 nm). In the report part, we chose x-y pairs and the actual option. After that, we selected the auto store tab and changed the autosave to ASCII(CSV). We press autozero after that and placed the cuvette in the holder and start our PL scan.

XRD: We prepared two samples for measuring by this device. Our samples were carbon quantum dots (CQDs) obtained from orange juice with 2 g thiourea that was filtered by vacuum, syringe, and centrifuge together (regular filter procedure) and the chromatography column. We dropped a little of them on the 1 cm × 1 cm lame for drying and we continue this way until achieving a thick sample on the lame.

They measured at 15-60 ˚C (2θ). Figure 4.17 and shows the XRD images of the sample that was filtered by chromatography column and RFP (regular filter procedure) respectively.

TEM: We prepared three samples for measuring by this device. Our samples were carbon quantum dots obtained from orange juice with 2, 1.5, and 0.3 g thiourea since according to their PL graph (Figure 4.18) they have different intensities in the 325 nm and 350nm excitation.

FTIR: We used this device for our six samples: three samples from orange juice with 2, 1.5, and 0.3 g thiourea and three samples from citric acid with the same amount of thiourea (Figure 4.19).

3. ENERGY

A band gap is the distance between the valence band of electrons and the conduction band. The band gap illustrates the minimum energy that is required to excite an electron up to a state in the conduction band where it can participate in conduction. The lower energy level is the valence band, and thus if a gap exists between this level and the higher energy conduction band, energy must be input for electrons to become free [32]. The energy of a photon is related to its frequency/wavelength is the formula of energy of the photon where h is Planck's constant and c is the speed of light, ν is the frequency.

$$E = \frac{hc}{\lambda} = h\nu \tag{3.1}$$

The amount of hc is constant (hc=1240 eV. nm)

Table 3.1 : Energy amounts of three samples of orange juice with different amounts of thiourea at different excitation wavelengths.

Excitation wavelength (nm)	Energy (eV)		
	Amount of thiourea		
	0.3 g	1.5 g	2 g
300	3.37	3.20	3.31
325	3.03	3.02	3.06
350	2.88	2.93	2.99
375	2.68	2.76	2.79
380	2.68	2.76	2.79
400	2.62	2.64	2.66
425	2.50	2.52	2.53
450	2.36	2.47	2.46

4. RESULT AND DISCUSSION

4.1 The Effect of Filtration and Doping Agent (thiourea)

In order to examine the effect of filtration (pulp-free) and doping of thiourea, absorption and PL spectra of pure orange juice (PO) and CQDs obtained from N- and S- doped orange juice (N, S-CQDs) were examined (Figure 4.1).

The absorbance spectrum shows that the absorption of the sample with filter and without thiourea is better than the pure sample without both of them, but the best result is for the sample with both filtration (pulp-free) and thiourea (0.1 g). In contrast, comparing the red and black lines and the blue lines in the PL plot, it is seen that doping has a significant effect. This shows us that with doping of surface passivation, a significant result can be achieved in PL emission intensity. Therefore, filtering has been found to be important.

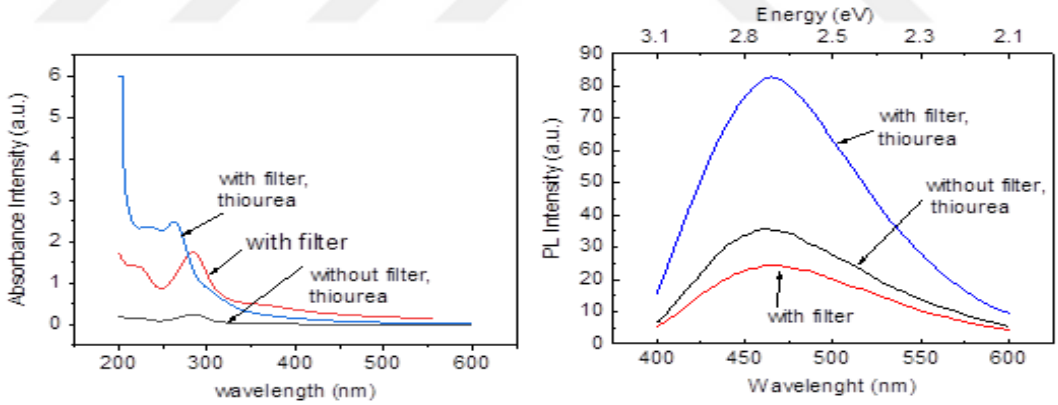

Figure 4.1 : Comparison of absorbance and PL spectra of PO and N, S-CQDs according to filtration procedure and effect of thiourea.

After realizing that filtration is crucial, the effect of different filtration methods was investigated further (Figure 4.2). In the PL spectroscopy graph, the regular filtration procedure (RFP) has a huge peak rather than other samples. When the PL emission spectra of the carbon dots obtained using the column chromatography filtering (CCF) method are examined, the fact that the maximum PL emission intensity at 454 nm is very low compared to RFP shows that the CCF method is not very suitable for filtering carbon dots.

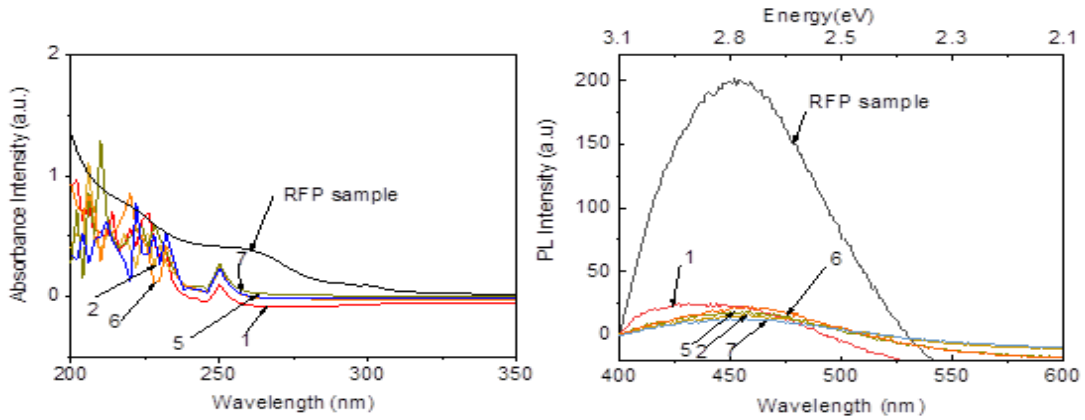

Figure 4.2 : Comparison of absorbance and PL spectra of the column chromatography samples (ten were taken sequentially) and RFP (vacuum, syringe, and centrifuge) sample obtained from N, S-CQDs doping with 2 g thiourea.

4.2 Ultraviolent Visible Near Infrared (UV-Vis-NIR) Spectroscopy

UV-Vis spectroscopy absorption of CQDs explores the optical characteristics of N, S-CQDs. In order to understand the role of thiourea, the UV-Vis absorption spectra of CQDs prepared by using different amounts of thiourea (0.05-2 g) with orange juice were investigated. (Figure 4.3). Absorbance intensities vary with increasing amounts of thiourea. However, it is increasing in general, except for some deviations.

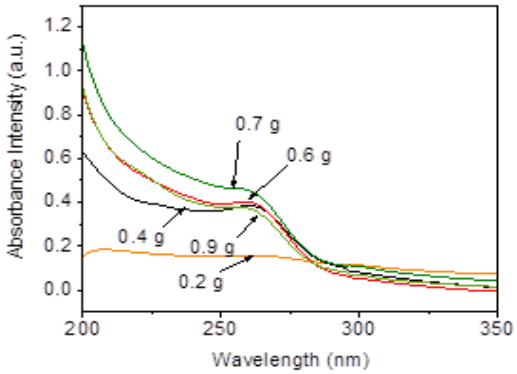

Figure 4.3 : Comparison of the UV-Vis spectra of CQDs obtained from different amounts of thiourea.

The peak less than 300 nm is assigned to the $\pi \rightarrow \pi^*$ transition of aromatic sp^2 domains of the conjugated C=C bands from a carbon core. Moreover, the UV absorption peak at wavelengths over 300 nm is attributed to the presence of $n \rightarrow \pi^*$ transition from C=O bands or other functional groups like NH_2 and SO_3H [12]. According to Figure 4.4, CQD samples containing 0.05, 0.1, 0.3, and 0.5 g of thiourea have two absorption shoulders below 300 nm, which can be assigned to the $\pi \rightarrow \pi^*$ transition. On the other

hand, in the CQD sample containing 2 g of thiourea, in addition to the π→π* transition, there is another peak at 301 nm, which can be attributed to the n→π* transition.

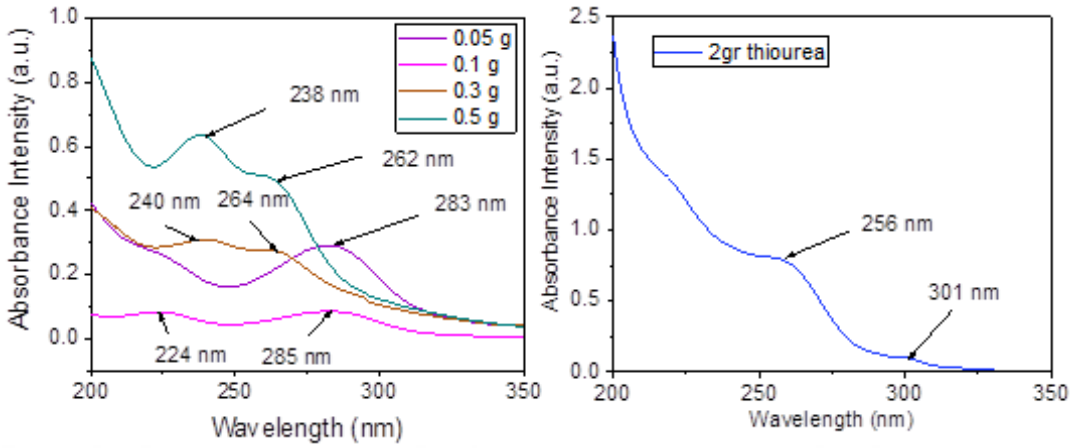

Figure 4.4 : π→π*and n→π* transition of UV absorption.

4.3 Photoluminescence (PL) Spectra

In the context of spectroscopy, the emission spectra refers to the output of a fluorophore at a specific wavelength, commonly referred to as the emission maximum [33, 34]. Conversely, the excitation maximum is the wavelength that excites the fluorophore [34].

Figure 4.5 depicts the photoluminescence spectroscopy of CQDs extracted from orange juice with varying concentrations of thiourea. The analysis shows an increase in photoluminescence intensity with an increase in the concentration of thiourea, as evidenced by the graph. The maximum fluorescence intensity is observed at 0.9 g thiourea.

In accordance with Figure 4.6, three samples of carbon quantum dots (CQDs) obtained from orange juice with varying amounts of thiourea (0.3, 1.5, and 2 g) were selected due to their distinct photoluminescence (PL) intensities at excitation wavelengths of 325 nm and 350 nm. The emission peak intensities were attributed to the n→π* transition of the C=O on the CDs. Also, the effect of thioura is obvious in the Figure 4.6 (d). Furthermore, Figure 4.7 displays the normalized PL intensity of CQDs obtained from orange juice and citric acid, using the same amounts of thiourea. These emission peaks, specifically the maximum peak, exhibited a slight shift towards longer wavelengths. Hence, Figure 4.7 demonstrates that the N, S-CDs are excitation-

dependent. As the excitation wavelength increased gradually from 300 to 450 nm, the maximum PL peak of the N, S-CQDs shifted from 367 to 527 nm (Figure 4.7(a)).

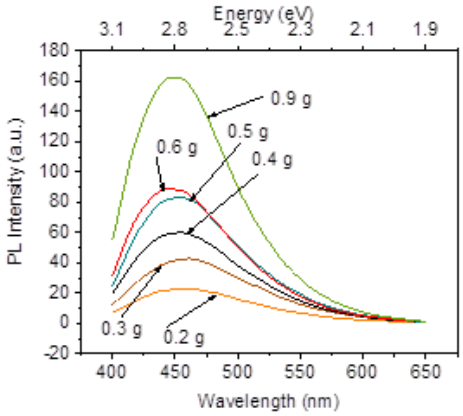

Figure 4.5 : PL spectroscopy of orange juice samples with different amounts of thiourea at 380 nm excitation.

In Figures 4.7 (b) and (c), the maximum PL peaks shifted from 388 to 502 nm and 377 to 502 nm, respectively, resulting in red shift. Similarly, Figures 4.7 (d) and (e) depict the normalized PL intensity of CQDs obtained from citric acids. At excitation wavelengths of 325 nm and 350 nm, the peaks were blue-shifted, while other excitations resulted in red-shifts in Figure 4.7 (d). Conversely, in Figure 4.7 (e), the peaks were blue-shifted at excitation wavelengths of 300 nm and 325 nm, while other excitations resulted in red-shifts. Additionally, Figure 4.7 (f) exhibited a red-shift. Tables 4.1 and 4.2 provide further information on these graphs.

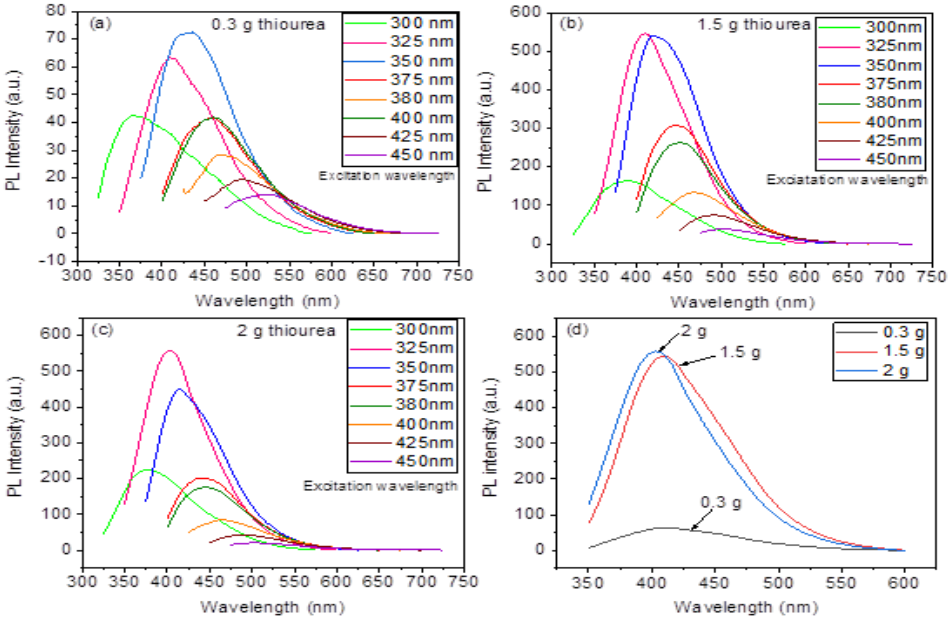

Figure 4.6 : PL spectroscopy of orange juice samples with (a) 0.3 g, (b) 1.5 g, and (c) 2 g thiourea (d) three certain amount of thiourea at 325 nm excitation.

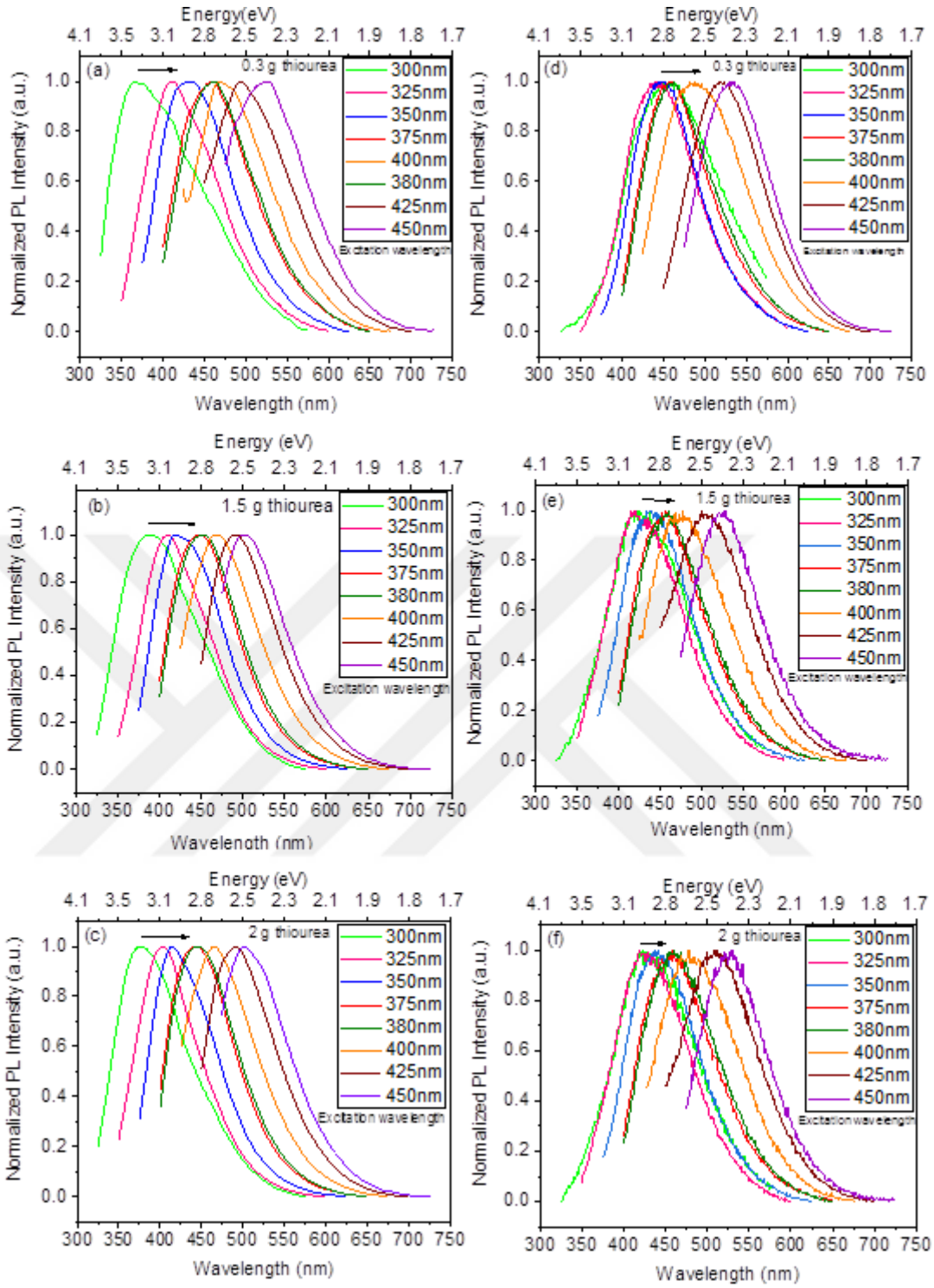

Figure 4.7 : Normalized PL intensity of orange juice samples with (a) 0.3 g, (b) 1.5 g, and (c) 2 g thiourea and citric acid samples with (d) 0.3 g. (e) 1.5 g, and (f) 2 g.

Table 4.2 indicates that the emission peak for the sample containing 0.3 g of thiourea under 325 nm excitation occurs at 441.95 nm, while for the sample containing 1.5 g of thiourea, it occurs at 418.92 nm, indicating a blue shift. Furthermore, Figure 4.8 reveals that increasing the amount of thiourea in the sample of citric acid results in a decrease in the PL intensity. The emission maximum for a fluorophore is always at a

longer wavelength, which corresponds to lower energy than the excitation maximum, and the difference between these two maxima is known as the Stokes shift [34] (Figure. 4.9). For example, the Stokes shift in the CDs obtained from orange juice containing 0.3 g of thiourea under 325 nm excitation is 85.29 nm (Figure. 4.9 (a)). Additionally, the Stokes shift is equal to the difference between the peak emission wavelength and the peak excitation wavelength [35] (Tables 4.1, 4.2, 4.3, and Figure. 4.10).

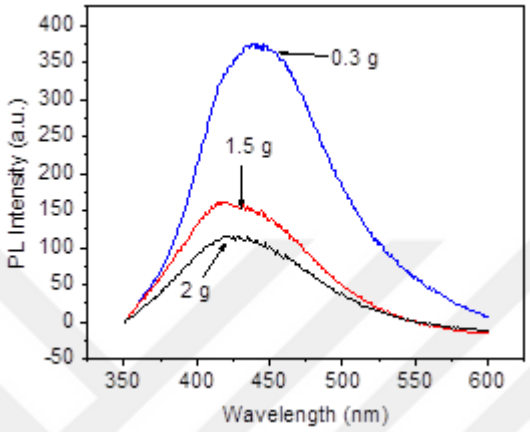

Figure 4.8 : PL spectra of CQDs obtained from citric acid with three certain amounts of thiourea at 325 nm excitation.

The Full Width at Half Maximum (FWHM) is a parameter commonly used to describe the width of a peak in a function or curve [36]. A larger FWHM value indicates a wider beam spread, which leads to more light diffusion [36]. Hence, lower FWHM values are preferred (Tables 4.2 and 4.3). Among the three orange juice samples, the FWHM value at 450 nm excitation wavelength is better. Generally, a large $FWHM_{abs}$, a small $FWHM_{em}$, and a large Stokes shift are advantageous for many bio-imaging applications since they allow for high-resolution and high-contrast bio-images [35]. As demonstrated in Figure 4.10 (a), the Stokes shift gradually decreases upon the addition of thiourea in the CDs samples from orange juice, whereas this is not the case for the CDs samples from citric acid. Furthermore, Figure 4.10 (b) illustrates the dependence of the FWHM value on the amount of thiourea in the CDs samples from orange juice; the FWHM value decreases as the amount of thiourea increases, and the FWHM values are narrower and lower than those of the CDs samples from citric acid.

In addition, the energy dependency can be deduced from Tables 3.1, 4.3, and 4.6, which indicate that as the exciting wavelength increases, the bandgap energies decrease for different amounts of thiourea. The excitation dependency is due to the presence of different functional groups with various band gap energy levels [35].

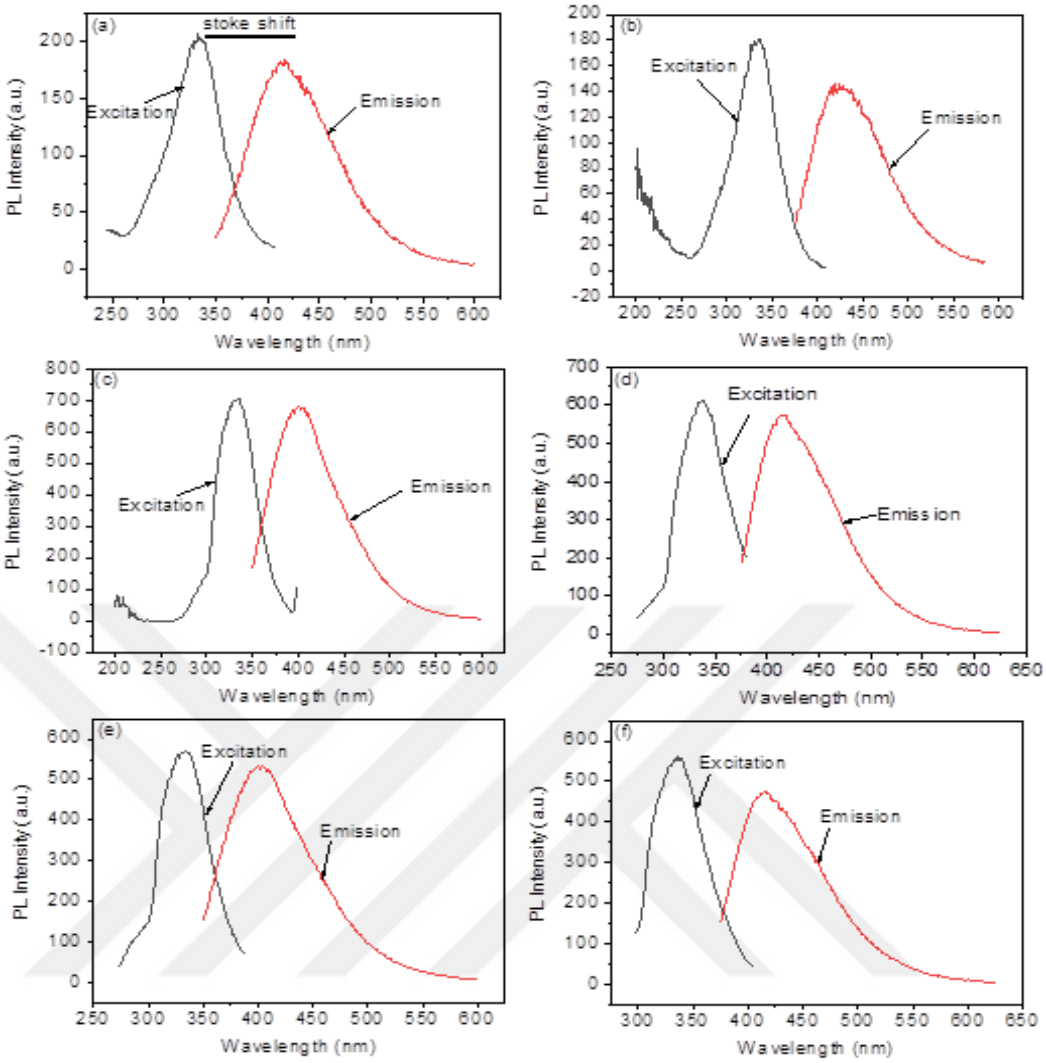

Figure 4.9 : Excitation and emission graphs of CQDs obtained from orange juice with (a), (b) 0.3 g thiourea at 325 nm and 350 nm, (c), (d) 1.5 g thiourea at 325nm and 350 nm, and (e),(f) 2 g thiourea at 325 nm and 350 nm excitation.

Table 4.1 : Stoke shift of CQDs obtained from orange juice with certain amounts of thiourea at different excitations.

Amount of thiourea (g)	CQDs obtained from orange juice	
	at 325 nm	at 350 nm
0.3	85.29	84.85
1.5	64.74	80.71
2	69.17	80.03

According to Figure 4.11, excitation-dependent emission properties of the six CDs species as obvious in the figure and by comparing the PL positions (symbols ●) of CQDs obtained from orange juice and citric acid. The excitation wavelengths ranging is from 300 nm to 450 nm. The emission peak position of all samples shifts to longer wavelengths resulting in an emission redshift.

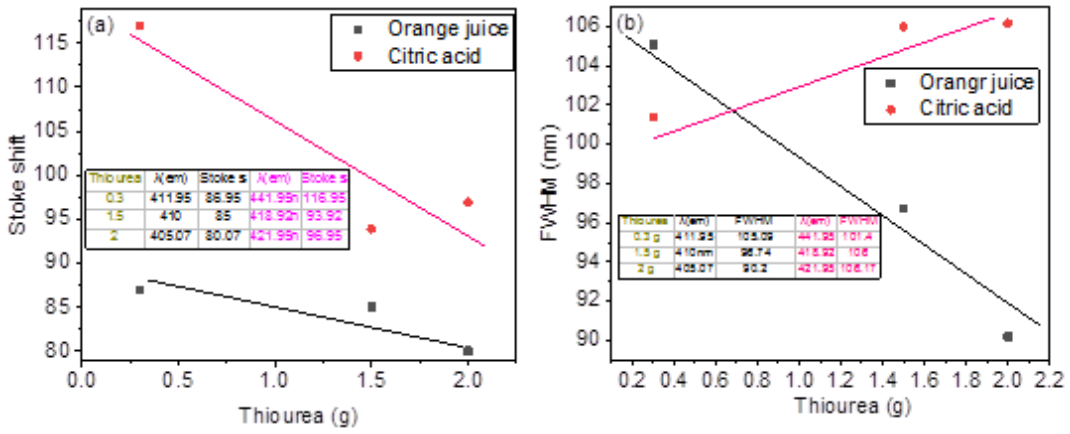

Figure 4.10 : (a) A linear correlation between the stokes shift and amounts of thiourea. (b) A linear correlation between the FWHM and amounts of thiourea.

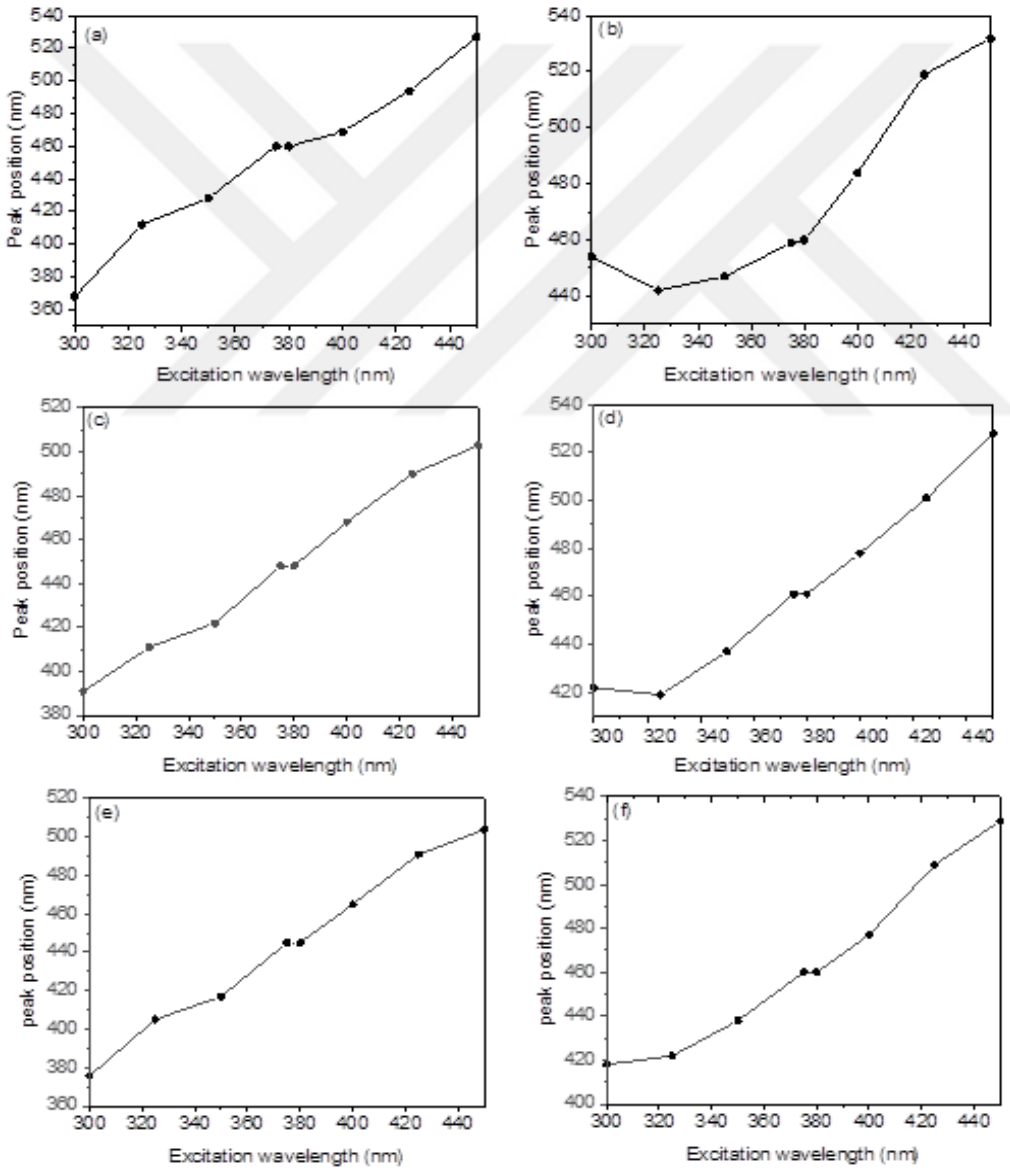

Figure 4.11 : PL peak position (●) as a function of the excitation wavelength for orange juice (a) 0.3 g, (c) 1.5 g. and (e) 2 g and citric acid (b) 0.3 g, (d) 1.5 g, and (f) 2 g with thiourea.

Table 4.2 : Optical properties CQDs obtained from orange juice with different amounts of thiourea.

Amount of thiourea (g)	UV-vis		PL			
	λ_{abs} (nm)	FWHM (nm)	λ_{em} (nm)	λ_{ex} (nm)	Stokes shift (nm)	FWHM (nm)
0.3	240	86.6459	367.83	300	67.83	128.22
	261	65.36	411.95	325	86.95	105.09
			428.29	350	78.29	111.94
			460	375	85	108.97
			460	380	80	109.71
			468.92	400	68.92	116.09
			494	425	69	115.01
			526.90	450	76.9	109.13
1.5	258	54.80172	390	300	86.92	117.18
	301	17.81749	410	325	85	96.74
			421	350	73	99.77
			448.02	375	76	93.76
			448.02	380	71	98.73
			468	400	68.92	102.40
			490	425	63.92	97.7
			502.98	450	52.98	86.15
2	257	50.14925	375.59	300	75.59	103.15
	300	13.65854	405.07	325	80.07	90.2
			416.96	350	66.96	93.97
			445	375	70	94.07
			445	380	65	96.05
			465	400	65	94.22
			491	425	66	97.9
			503.88	450	53.88	88.42

Table 4.3 : Optical properties of CQDs obtained from citric acid with different amounts of thiourea.

Amount of thiourea with 0.32 g citric acid (g)	PL				Energy (eV)
	λ_{em} (nm)	λ_{ex} (nm)	Stokes shift (nm)	FWHM (nm)	
0.3	454	300	154	130.89	2.73
	441.95	325	116.95	101.4	2.8
	446.95	350	96.95	95.18	2.77
	458.95	375	83.95	98.82	2.7
	460	380	80	101.81	2.69
	483.92	400	83.92	123.75	2.56
	518.95	425	93.95	106.84	2.38
	531.94	450	81.94	104.67	2.33
1.5	421	300	121	115.38	2.94
	418.92	325	93.92	106	2.95
	436.95	350	86.95	99.76	2.83
	461	375	86	101.77	2.68
	461	380	81	102.06	2.68
	478	400	78	115.27	2.59
	501	425	76	117.07	2.47
	528.88	450	78.88	100.98	2.34
2	418	300	121.95	115.93	2.93
	421.95	325	96.95	106.17	2.93
	438	350	88	100.87	2.83
	460	375	85	103.96	2.86
	460	380	80	108.06	2.86
	477	400	77	114.55	2.59
	508.95	425	83.95	114.23	2.43
	528.96	450	78.96	97.53	2.34

4.4 Quantum Yield (QY)

The efficiency of photon emission, as defined by the ratio of the number of photons emitted to the number of photons absorbed, is referred to as the quantum yield (QY) [23]. In order to measure the photoluminescence (PL) brightness, QY is determined. Quinine sulfate ($C_{40}H_{50}N_4O_8S$) is commonly used as a fluorescence standard due to its PL excitation and emission wavelength similar to carbon dots (CDs). Among various parameters affecting QY, particle size is regarded as one of the most crucial factors [23]. In particular, an increase in particle size is generally found to reduce the QY efficiency. Moreover, doping with nitrogen (N) and sulfur (S) atoms can enhance QY by improving the emission through a fluorescence-enhancing effect [37].

In this study, we observed that the particle size of CQDs synthesized using the microwave-assisted method was generally large, leading to decreased QY values. Furthermore, we found that the addition of thiourea as a doping agent to the carbon source could reduce the particle size and increase the QY. To determine QY, absorbance and PL intensity were measured and plotted against quinine sulfate (QY=0.54) as a reference in 0.1 M H_2SO_4. The equation used to calculate QY is provided below (Eq. 4.1). Finally, the results presented in Figure 4.18 demonstrate a significant increase in QY with the addition of thiourea as a doping agent. The subscripts "s" and "r" are for carbon dots and quinine sulfate as a reference, respectively.

$$QY_s = QY_r \frac{I_s}{I_r} \times \frac{A_r}{A_s} \times \left(\frac{\eta_s}{\eta_r}\right)^2 \quad (4.1)$$

"I" corresponds to the integrated PL intensity, "A" corresponds to the absorbance measured at the excited wavelength, and "η" refers to the solvent refractive index (1.33).

In this study, stock solutions were prepared with 10^{-3} M of quinine sulfate dissolved in 0.1 M H_2SO_4. In order to prevent errors resulting from self-absorption, a series of standard solutions were prepared at concentrations lower than 10^{-3} M by diluting the reference stock solution to have an absorbance of 0.1 and less than 0.1. In addition, a series of samples of CDs that are orange juice with different amounts of thiourea (0.3, 1.5, and 2 g) were prepared where their absorbances were lower than 0.1 at 325 nm. Then measured their PL intensities with an excitation of 325 nm were integrated. QY

of the orange juice samples with 0.3, 1.5 and 2 g thiourea were 2.4 %, 5.9 %, and 7.1 %, respectively (Figure 4.12).

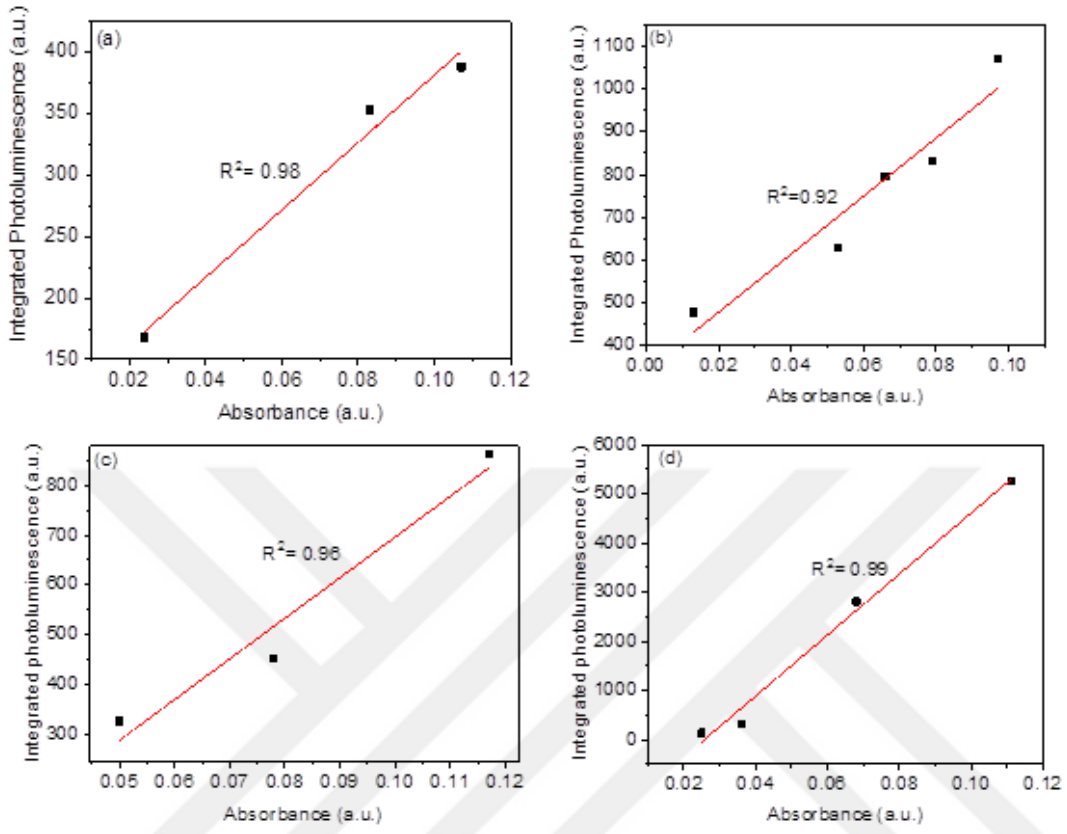

Figure 4.12 : The integrated PL emission intensity of the orange juice samples with (a) 0.3 g, (b) 1.5 g, and (c) 2 g thiourea and (d) quinine sulfate as a reference.

Table 4.4 : Comparison of QY values of CQDs obtained by using citric acid-containing fruits with different parameters (synthesis method, time, power used and temperature).

Precursor	Doped atom	Method	Time (min)	Power / Temperature	QY (%)	Ref.
Strawberry J	N	HT	720	180 ºC	6.3	[38]
Lemon J	-	HT	720	150 ºC	21.37	[39]
Lemon J	-	MW	5	800 W	0.74	[40]
Grapefruit J	N, S	HT	360	180 ºC	84.93	[41]
Orange J	-	HT	150	120 ºC	26	[42]
Orange J	N, S	MW	15	800 W	7.1	in this study
Tomato	-	HT	360	180 ºC	9.7	[43]
Pomelo	N, S	HT	300	180 ◦C	17.31	[44]
Pineapple	-	HT	360	200 ◦C	10.65	[45]

HT: Hydrothermal, MW: Microwave, Juice: J

Table 4.4 presents the quantum yield (QY) data of citric acid-containing fruits utilized in prior studies to synthesize carbon quantum dots (CQDs). This table compares the QY values obtained from diverse synthesis methods and factors such as time, power, or temperature. The highest QY value of 84.93% was attained from grapefruit juice via hydrothermal synthesis with nitrogen (N) and sulfur (S) doping. In contrast, the lowest QY value of 0.74% was achieved through the microwave-assisted method without surface passivation. Despite the frequent use of the hydrothermal method for CQD synthesis in the literature, there are limited studies on microwave-assisted synthesis methods. Therefore, in this thesis, the microwave-assisted method was preferred since it allows for homogeneous heat distribution and very short time CQD synthesis (at 800 W, 15 min). Remarkably, the QY value of CQDs synthesized from orange juice by doping with N and S is more promising than those attained from hydrothermal techniques for a longer duration, such as strawberry juice [38], tomato [43], and pineapple [45]. Hence, microwave-assisted techniques can save time and offer homogeneous heating, making them a viable alternative to traditional methods.

4.5 3D Graphs of Emission and Excitation

Interestingly, it is quite clear from the 3D contour map that the effects of thiourea doping in orange juice and citric acid on the PL emission intensities are opposite to each other (Figure 4.13). According to Ludmerckzi et al. [46], the oblique lines also observed in the 3D contour map graphs are due to particle scattering effects. The effect of the excitation wavelength and thiourea amounts (0.3, 1.5, and 2 g) on the PL emission intensity from Figures. 4.13 (a) to (c) increases with a maximum at 400 nm in the red region, when excited at 330 nm. The PL emission of these samples (orange juice with different amounts of thiourea) is dependent on the excitation wavelength. From Figures. 4.13 (d) to (f), the maximum emission wavelength shifts dramatically from 450 to 430 nm. In addition, the 3D contour map graph in Figure 4.13 (d) indicates the presence of three components. In the first one, emission increases with a maximum of 450 nm in the red region when excited at 350 nm. Moreover, the second one is in the blue region, the PL emission of which peaks at around 480 nm with an excitation of 270 nm, and the third one PL emission wavelength shifts to 520 nm with an excitation of 430 nm. The PL emission of these samples (citric acid with different amounts of thiourea) is also dependent on the excitation wavelength. According to

Figure 4.13 (f), surprisingly, the PL emission intensity is completely quenched probably due to the formation of hydrogen bonds with water on the surface (Figure 4.8).

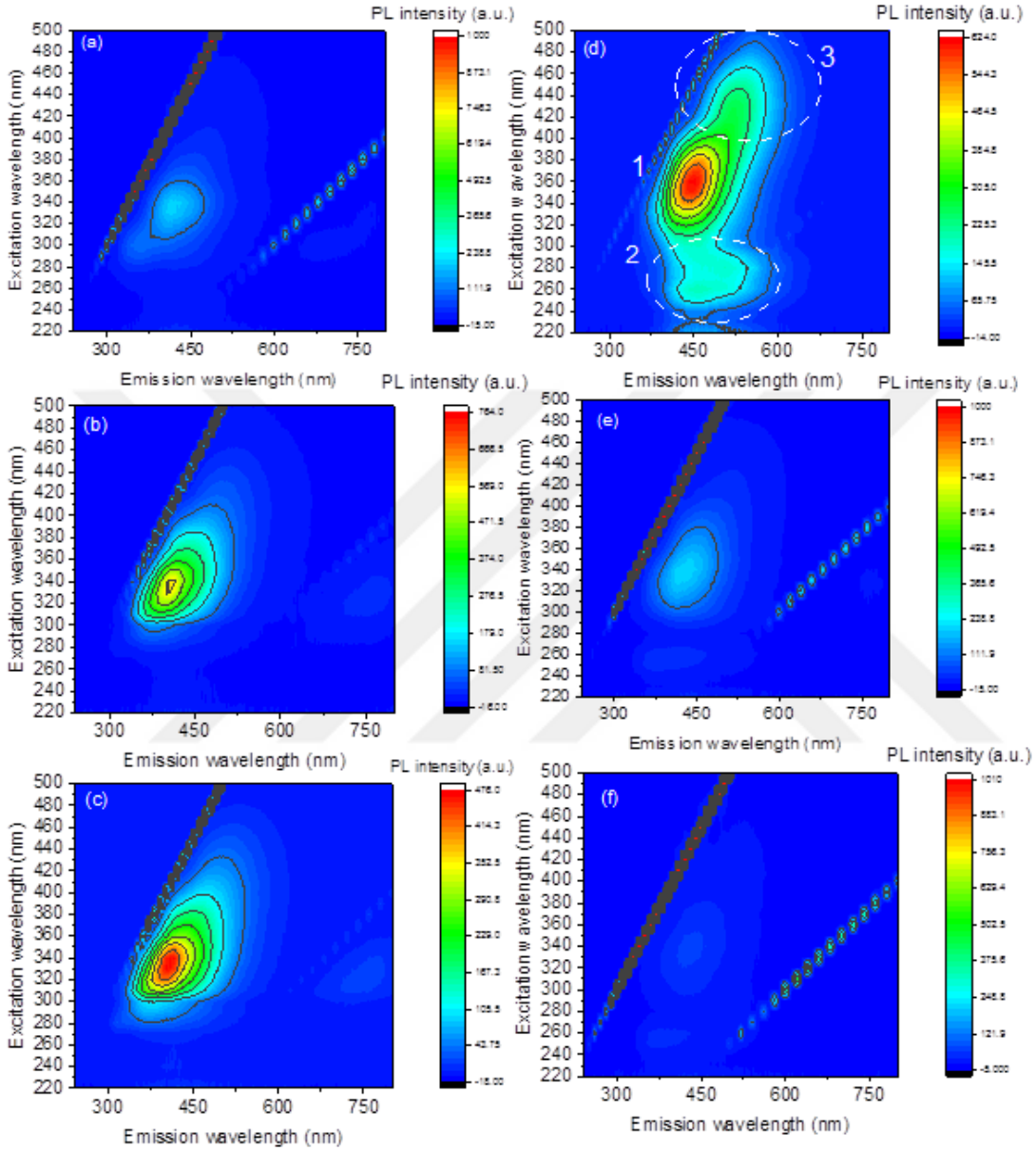

Figure 4.13 : 3D excitation-emission-intensity spectra of orange juice with (a) 0.3 g, (b) 1.5 g, and (c) 2 g thiourea and citric acid with (d) 0.3 g, (e) 1.5 g, and (f) 2 g thiourea.

4.6 Solvent Effect

The solubility of carbon-based nanomaterials like carbon nanotubes, fullerenes, and graphene in water is weak. In addition, they have a strong shortcoming of fluorescence in the visible area. However; CQDs can take part in the chemiluminescence reaction

as oxidants, emitting species, and energy acceptors of chemical reactions. CQDs are also comfortably dispersed in protic and aprotic solvents owing to carboxyl, hydroxyl, and carbonyl groups [47].

In this study, CQDs obtained from orange juice doped with thiourea using microwave-assisted synthesis dispersed easily in protic (ethanol, methanol) and aprotic (acetonitrile, and acetone) solvents, but they cannot disperse in the non-polar solvents like chloroform and n-hexane. The interaction between carbon dots and solvents has a vital role in the wavelength of photoluminescence emissions. The effect of the solvent on fluorescence depends on both its polarity and the nature of the carbon dots. Although the absorption of CQDs is independent of the nature of the solvent, their PL spectra are significantly dependent on it since there are functional groups on the carbon dots' surface that are available to solvent molecules. Therefore, strong interactions of carbon dots with solvent molecules can have a significant effect on fluorescence. However, fluorescence properties are complicated owing to dependence on excitation wavelength and solvent nature. Different parameters such as hydrogen bonding ability and polarization of dipole moment are considered in the determination of solvent-solute interaction and solvent environments.

Identifying the dipole moment of electron balances is important because it can illustrate how electron distribution alters under excitation [47]. Through the process of absorption, the energy fluorophore undergoes excitation to attain a higher energy state, thereby entering a state of greater energy. There will be an alteration in the dipole moment. Moreover, solvent relaxation occurs when the dipole moment of the surrounding solvent reduces the energy of the excited state of the fluorophore, affecting molecules, causing a red shift in the wavelength. Furthermore, when the polarity of the solvent is increased, the energy level of the excited state is decreased. In non-polar solvents, the excited state of the fluorophore is unstable, thus producing a correspondingly larger energy gap between the ground and excited states [48].

Table 4.5 : The value of FWHM of CQDs obtained from orange juice and three certain amounts of thiourea, which dissolved in different polarity solvents.

	Amount of thiourea (g)	Excitation wavelength (nm) 300	325	350	375	400	425	450	Relative Polarity [49,50]	Dipole moment [50,51]
		FWHM								
W	0.3	128.22	105.09	105.51	111.32	109.63	111..95	109.12	1	1.84 D
	1.5	117.18	96.74	99.77	93.76	94.87	97.7	83.83		
	2	103.16	90.02	93.97	91	94.22	93.78	88.42		
M	0.3	149.26	95.03	98.3	104.81	107.41525	108.26	96.64	0.762	2.8 D
	1.5	117.18	90	93.11	90.19	99.13	104.26	92.79		
	2	112.68	90	90.86	92.43	100.32	106	98.31		
E	0.3	123.41	87.41	91.18	102.69	110.27	114.43	97.51	0.654	2.37 D
	1.5	103.05	85.2	89	99.23	112.71	105.1	91.62		
	2	118.8	89.85	92.39	103.03	112.67	104.97	97.77		
AN	0.3	130.9	86.45	93.72	109.91	112	112.78	108.52	0.46	3.44 D
	1.5	101.75	82.62	84.66	98.68	110.9	104.22	94.06		
	2	118.79	84.66	93.17	104.61	116.02	105.052	95.67		
A	0.3	210.63	94.76	97.86	104.43	102.17	107.54	100.81	0.355	2.69 D
	1.5	196.21	88.47	95.62	92.96	108.17	105.84	96.73		
	2	206.99	94.76	100.81	94.99	113.12	103.03	91.86		
C	0.3	90.16	79.16	92.91	98.81	100.943	99.05	97.51	0.259	1.15 D
	1.5	108.83	95.03	102.82	100.88	97.91	100.54	75.81		
	2	148.53	133.38	113.65	103.05	101.63	101.61	96.26		
NH	0.3	231.34	94.76	231.34	94.76	100.81	107.54	103.24	0.009	0.08 D
	1.5	57.98	53.34	57.98	53.34	76.37	64.53	41.09		
	2	55.76	42.78	55.76	42.78	43.95	64.13	98.98		

Water, M: Methanol, E: Ethanol, AN: Acetonitrile, A: Acetone, C: Chloroform, and NH: N-hexane.

Table 4.6 : The energy of CQDs that was dissolved in three different kinds of solvents.

Solvents	Amount of thiourea (g)	Excitation wavelength (nm)						
		300	325	350	375	400	425	450
		Energy (eV)						
C	0.3	3.13	3.15	3	2.83	2.66	2.53	2.44
	1.5	3.02	3.02	2.98	2.76	2.66	2.51	2.50
	2	2.53	2.69	2.63	2.66	2.58	2.48	2.42
A	0.3	3.28	3.05	2.98	2.70	2.65	2.54	2.39
	1.5	3.04	3.01	2.96	2.79	2.60	2.48	2.40
	2	3.03	3.09	2.97	2.81	2.78	2.45	2.41
M	0.3	3.43	2.98	2.93	2.79	2.62	2.48	2.38
	1.5	3.14	3.06	2.96	2.69	2.80	2.47	2.41
	2	3.26	3.10	3	2.79	2.67	2.48	2.40

From Table 3.1, it can be deduced that as the exciting wavelength increases, bandgap energies decrease for different amounts of thiourea due to the redshift of the emission wavelength according to the results of Table 4.2.

CQDs prepared using different thiourea amounts were examined in different solvents (acetone, chloroform, and methanol) (Table 4.6). Obviously, as the exciting wavelength increases, bandgap energies decrease for different amounts of thiourea, which had different solvents because it is noticeable that the results in red-shift actions. Also, this reduction in energy gaps of carbon dots with increasing the solvent polarity (Tables 4.5 and 4.6) is assignable to the positive fluorescence solvatochromism [51] (solvatochromism could be a reversible alter of the absorption or outflow range of a fabric that's actuated by the activity of solvents [51]), which is related to the carbon dots from aromatic compounds shifted to the longer wavelengths as the solvent polarity increases (Figure 4.15, Table 4.7) [51]. According to the Figure 4.14, we selected solvents such as methanol (M), ethanol (E), acetonitrile (AN), and chloroform (C) to admit that stokes shift and emission energy are linearly dependent on empirical polarity parameter E_T (30) [52].

From Table 4.5, it is obvious that full width at half-maximum (FWHM) values change for each solvent which shows that these values are solvent-dependent. In addition, when these values are compared in their group, we notice that they have undercharged thiourea amounts. The maximum values of FWHM of three samples of water are at the 300 nm excitation and the minimum values are at the 450 nm excitation. Some of the other solvents have maximum values of FWHM on the 300 nm excitation. The results of chloroform show that the samples with 1.5 and 2 g thiourea have maximum

FWHM values on 300 nm excitation and minimum values on 450 nm excitation. In contrast, the results of the n-hexane solvent are not similar to others. In ethanol and methanol solvents with 0.3 and 2 g thiourea, the minimum values of FWHM are on 325 nm excitation. Figure 4.15 (b) shows the PL emission of CQDs doped with the thiourea in different solvents at 325 nm excitation, PL intensities decrease from water to n-hexane.

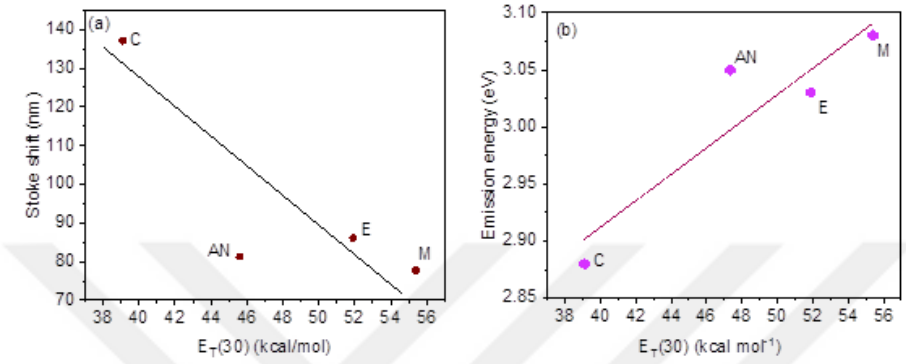

Figure 4.14 : (a) A linear correlation between the Stokes shift and empirical polarity parameter. (b) A linear correlation between the emission energy and polarity parameter.

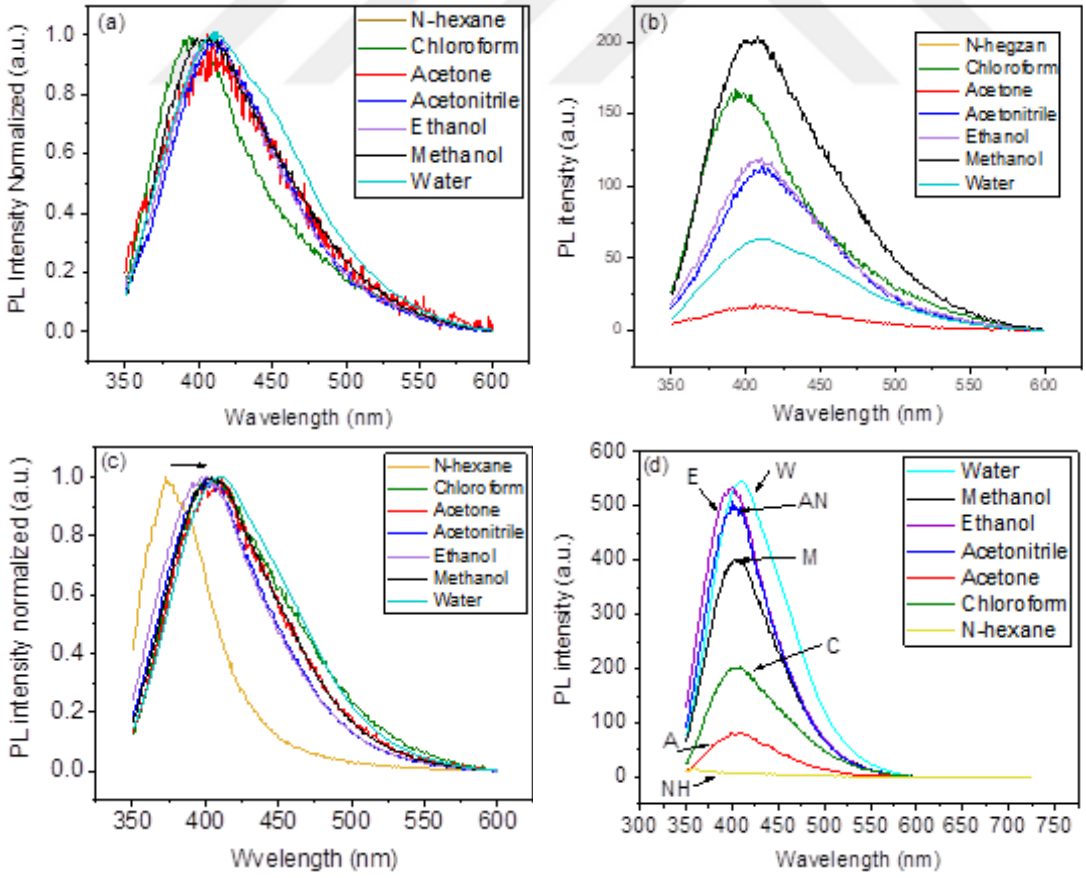

Figure 4.15 : The effect of different solvents environment on CQDs doped with thiourea 0.3 g (a), (b) and 1.5 g (c), (d) at 325 nm excitation.

According to Table 4.7, by increasing the polarity (n-hexane to water) the emission peak shifts to a longer wavelength [53]. However, according to Figure 4.16. the PL emission intensity decreases with increasing solvent polarity when the excitation wavelength is greater than 325 nm. In contrast, PL emission intensity increased with the active role of functional groups in the core of CDs at excitation wavelengths lower than 325 nm excitation apart from acetone, (λ_{ex} is >350 nm), and chloroform (λ_{ex} is > 425 nm).

Table 4.7 : Emission peaks of CQDs obtained from orange juice with different amounts of thiourea (excitation 325 nm) which were dissolved in the different solvents with different polarities.

Solvents	λ_{em} (nm) Thiourea (g)		
	0.3	1.5	2
N-hexane	405.71	359.67	364.33
Chloroform	393.03	399.2	462.11
Acetone	406	399.2	405.52
Acetonitrile	411.06	400.17	406.29
Ethanol	411.06	401.04	408.80
Methanol	408	407.94	402.80
Water	415	411.22	402.80

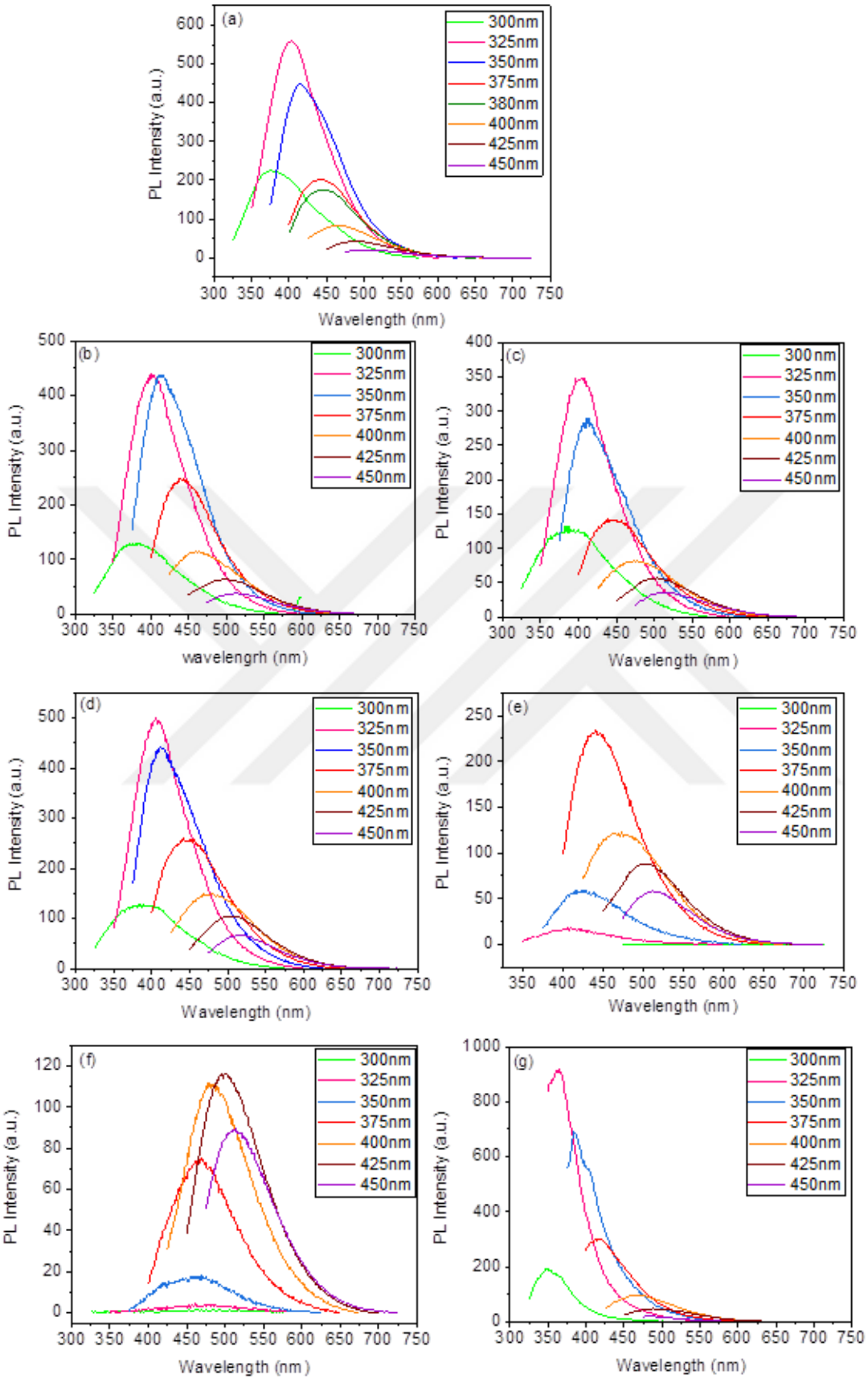

Figure 4.16 : The PL intensity of orange juice samples with 2 g thiourea were dissolved in (a) water, (b) methanol, (c) ethanol, (d) acetonitrile, (e) acetone, (f) chloroform, and (g) n-hexane.

4.7 X-Ray Diffraction (XRD)

The interaction of the incident X-rays with the sample produces constructive interference and a diffracted X-ray when conditions satisfy Bragg's law:

$$n\lambda = 2d\sin\theta \qquad (4.2)$$

where n is an integer, λ is the wavelength of the X-rays beam, θ is the diffraction angle, and d is the distance between the atomic layers in a crystal [54]. Figure 4.17 shows the XRD patterns of CQDs gained from orange juice with 2 g thiourea that was filtered by different methods. The black line was obtained using a chromatographic column filter, and the red line was obtained using an RFP method. Their peaks are at 23.89˚ and 28.30˚, respectively, of which both are corresponding to (002) hkl plane [53], and the d value of both of them is 0.36 nm and 0.32 nm respectively. 0.36 nm is larger than the graphitic interlayer spacing (0.34 nm), providing that the nature of CQDs has a weak crystalline structure [6,54]. Therefore, the results obtained by the RFP method according to the lattice parameters are more reasonable.

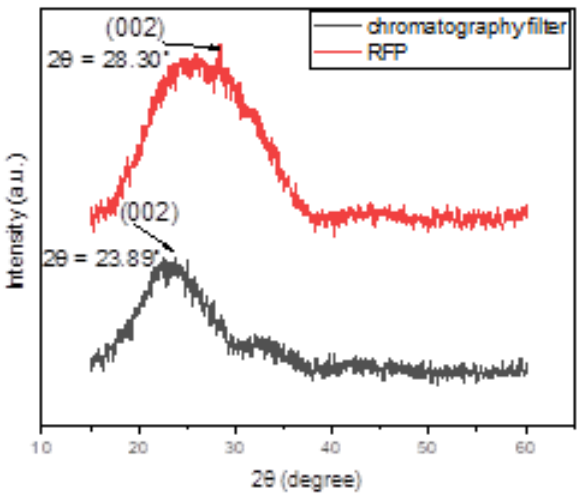

Figure 4.17 : XRD patterns of CQD using chromatography filter and RFP with 2 g thiourea.

4.8 Transmission Electron Microscopy (TEM)

By imaging with TEM, a beam of high-energy electrons is passed through a carbon dots sample, a part of the beam is transmitted and this part when projected on a fluorescent screen. As a result, TEM images are gained (Figure 4.18). Using Image J software, CQD particle size analysis was performed and distribution histograms were drawn.

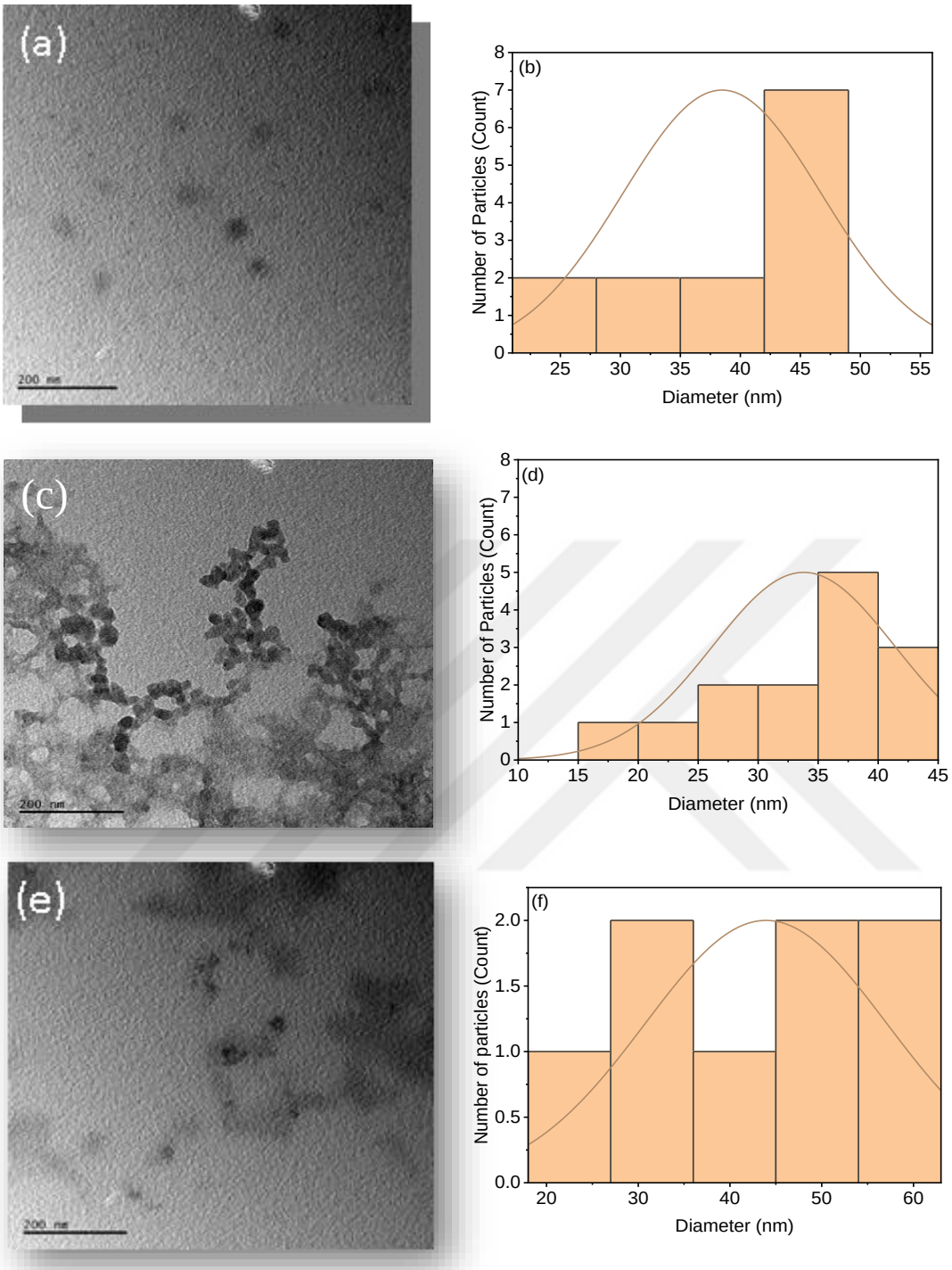

Figure 4.18 : TEM images (a, c, e) and their corresponding histograms of orange juice samples with thiourea 2 g (b), 1.5 g (d), 0.3 g (f).

It is impossible to observe the additional features like‘d’ spacing or fringe formations or defects in the structure of CQDs with images obtained by TEM analysis probably due to resolution and image phase contrast. According to Figure 4.18, by increasing the amount of thiourea the size of particles becomes smaller. Therefore, it can be said that the QY increases as the particle size decreases. The average diameter of the CQDs

in samples with 2 g and 1.5 g thiourea is approximately the same, around 30-50 nm, whereas, for the sample with 0.3 g thiourea, it is approximately 45 nm.

4.9 Fourier Transformation Infrared Spectroscopy (FTIR)

FTIR is employed for the identification of components and functional groups present on the surface of CQDs. It has been confirmed from the FTIR spectra that the CQDs have functional groups on their surface, which ensures their solubility in various solvents (Tables 4.5 and 4.8).

Table 4.8 : Identification of different species and their band adsorption observed from the FTIR spectrum [55-60].

Wavenumber (cm^{-1})	**Assignment***
3400-3200	ν_s (O-H)
3400-3200	ν_{as} (N-H)
2200-2000	ν (C≡N)
1680-1620	ν (C=C)
1700-1600	ν (C=O)
1200-1100	ν (C-S)
1200-1100	ν_{as} (C-O-C)
900-669	aromatic out of plane □ (C-H)

*ν = stretching, □ = bending, s = symmetric, and as = asymmetric.

FTIR spectrum of two samples (orange juice or citric acid) with different amounts of thiourea (0.3, 1.5, and 2 g) was shown in Figure 4.19 and 4.20 (a) and (b). In the FTIR spectrum, there are hydrophilic groups such as symmetrical and asymmetrical stretching of O-H and N-H peaks at 3200-3400 cm^{-1} [55, 56]. In addition, the peaks at around 2070-2154 cm^{-1}, correspond to the stretching of C≡N [57]. Meanwhile, the peaks at 1633-1640 cm^{-1} are attributed to the stretching vibration of the C=C and C=O groups [56, 58].

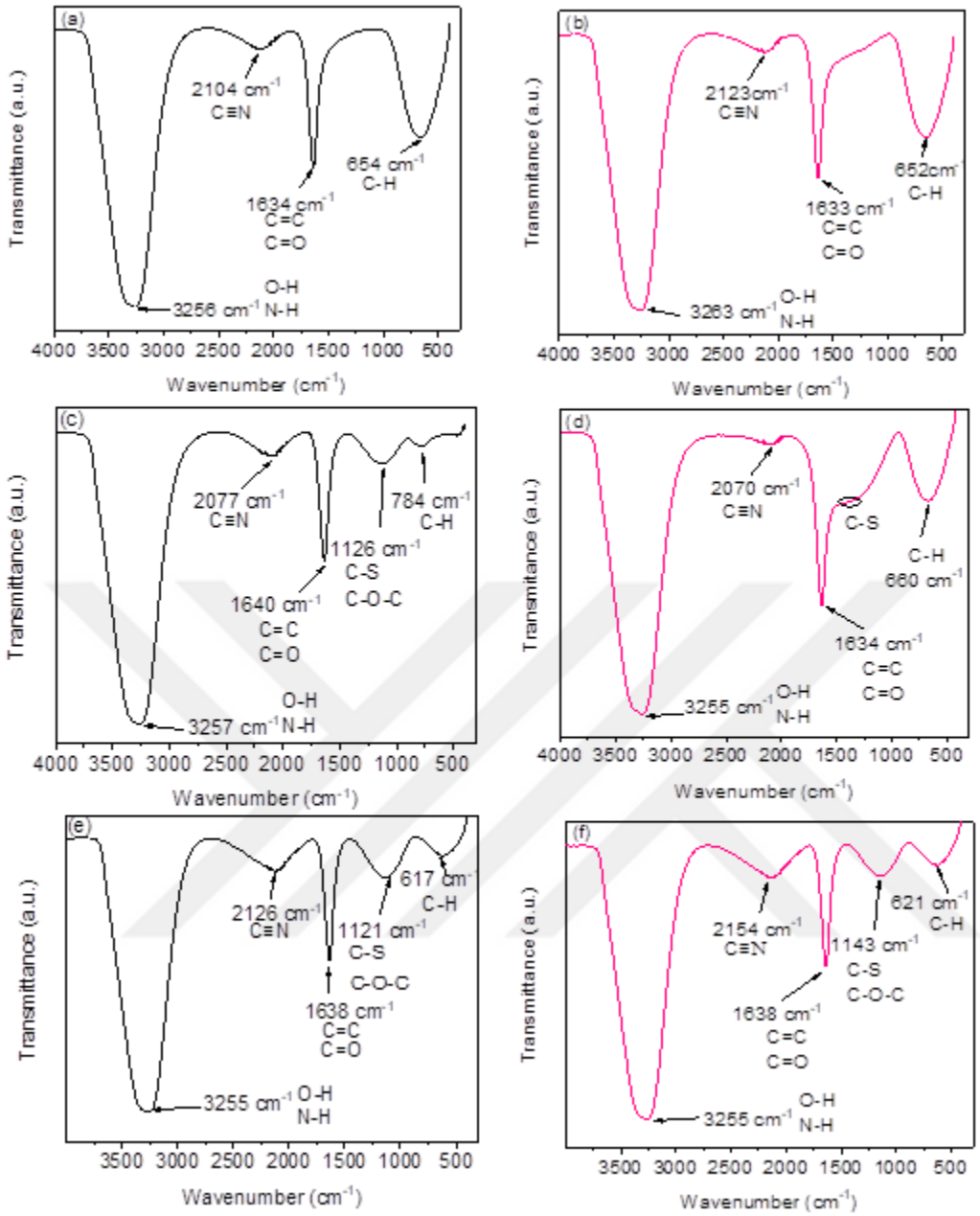

Figure 4.19 : FTIR spectrum of N, S doped carbon dots derived from orange juice with (a) 0.3 g, (c) 1.5 g, and (e) 2 g thiourea and from citric acid with (b) 0.3 g, (d) 1.5 g, and (f) 2 g thiourea.

The effect of the amount of thiourea doping is visible in the FTIR spectra. In Figure 4.19 (b), 4.20 (b) and (c), it is observed that a small peak starts the band at 1100-1200 cm^{-1}, where the C-S bond and asymmetric stretch C-O-C groups are present [55, 59]. Interestingly, this peak becomes more pronounced with an increase in the amount of thiourea. On the other hand, the bands belonging to these stretching vibrations are not observed in Figure 4.19 (a), 4.20 (a), and (c) yet, but with the increase in the amount of thiourea, these stretching vibrations begin to occur clearly in Figure 4.19 (c) and 4.20 (a). With the formation of these stretching vibrations, the decrease in the aromatic

out-of-plane C-H bending vibrations in the 669-900 cm^{-1} spectral region [60] proves the incorporation of sulfur into the structure of the CQDs.

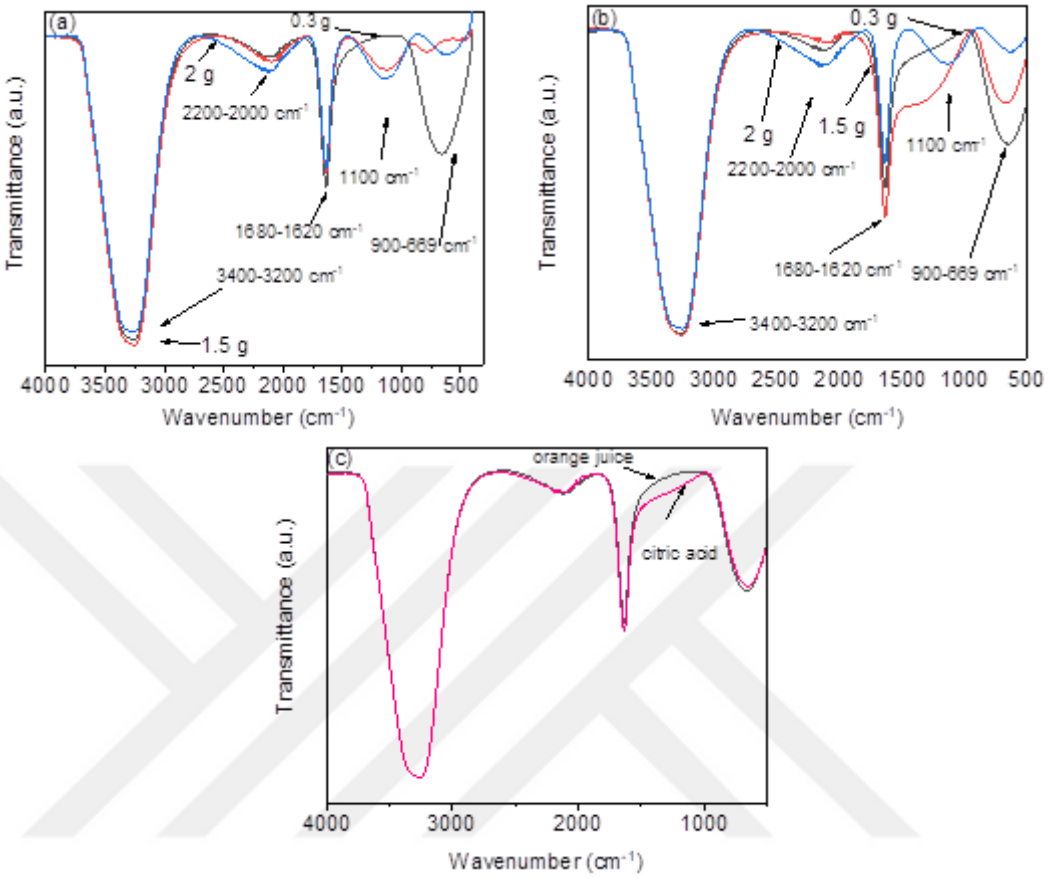

Figure 4.20 : FTIR spectrum of CQDs obtained from (a) orange juice and (b) citric acid with certain amounts (gram) of thiourea (c) orange juice and citric acid with 0.3 g thiourea.

5. CONCLUSION

This study reports on the synthesis and characterization of carbon dots that were synthesized successfully from orange juice with different amounts of thiourea through a microwave heating approach, which can be avoiding wasting time, and the heating of microwave techniques is homogenous. In addition, this method is a green, cheap, and simple approach.

We investigated the optical, structural, and in situ properties of the CQDs. After, detecting the effect of N, S- doping on the optical properties of CQDs, we selected three samples of c-dots with (0.3, 1.5, and 2 g) thiourea due to their PL spectra graphics. The spherical shape of the carbon core structure CQDs obtained from orange juice provided NS/CQDs with remarkable QY. Therefore, we synthesized CQDs by citric acid and these certain amounts of thiourea for comparison to the acting of the thiourea. By adding thiourea in the samples with citric acid, PL intensity decreases due to the formation of hydrogen bonds with water on the surface.

Also, the size distributions and average diameters of CQDs achieved from orange juice were obtained by TEM analyses.

Carbon dots fabricated in this study exhibited strong excitation-depend and solvent-depend properties. As the excitation wavelength changed the emission wavelength changed. The solvent polarity increased the PL emission wavelength shifted to a longer wavelength (redshift), which is positive fluorescence solvatochromism.

XRD analyses indicated the amorphous nature of carbon dots. Moreover, FTIR spectroscopy identified chemical bonds in a molecule and functional groups and indicated the effect of the amount of thiourea doping. C-S and C-H are chemical groups that have an effective role in our synthesis system.

REFERENCE

[1] **He, M., Zhang, J., Wang, H., Kong, Y., Xiao, Y., & Xu, W.** (2018). Material and Optical Properties of Fluorescent Carbon Quantum Dots Fabricated from Lemon Juice via Hydrothermal Reaction. Nanoscale Research Letters, 13.

[2] **Kaczmarek, A., Hoffman, J., Morgiel, J., Mościcki, T., Stobiński, L., Szymański, Z., & Małolepszy, A.** (2021). Luminescent carbon dots synthesized by the laser ablation of graphite in polyethyleneimine and ethylenediamine. Materials, 14(4), 1–13. https://doi.org/10.3390/ma14040729

[3] **Sharma, A., & Das, J.** (2019). Small molecules derived carbon dots: Synthesis and applications in sensing, catalysis, imaging, and biomedicine. Journal of Nanobiotechnology, 17(1), 1–24.

[4] **Wang, Y., & Hu, A.** (2014). Carbon quantum dots: Synthesis, properties, and applications. Journal of Materials Chemistry C, 2(34), 6921–6939.

[5] **Zhou, Y., Desserre, A., Sharma, S. K., Li, S., Marksberry, M. H., Chusuei, C. C., Blackwelder, P. L., et al.** (2017). Gel-like Carbon Dots: Characterization and their Potential Applications. ChemPhysChem, 18(8), 890–897. https://doi.org/10.1002/cphc.201700038

[6] **Singh, I., Arora, R., Dhiman, H., & Pahwa, R.** (2018). Carbon quantum dots: Synthesis, characterization and biomedical applications. Turkish Journal of Pharmaceutical Sciences, 15(2), 219–230.

[7] **Dutta, G. K., & Karak, N.** (2022). Overview of carbon dot synthesis. Carbon Dots in Agricultural Systems: Strategies to Enhance Plant Productivity, 39–68.

[8] **Rocco, D., Moldoveanu, V. G., Feroci, M., Bortolami, M., & Vetica, F.** (2023). Electrochemical Synthesis of Carbon Quantum Dots. ChemElectro Chem, 2022.

[9] **Hong, J., Kim, M., & Cha, C. (2019).** Multimodal carbon dots as biosensors. In Theranostic Bionanomaterials. Elsevier Inc.

[10] **Siahcheshm, P., & Heiden, P. (2023).** High quantum yield carbon quantum dots as selective fluorescent turn-off probes for dual detection of Fe2+/Fe3+ ions. Journal of Photochemistry and Photobiology A: Chemistry, 435(March 2022), 114284.

[11] **Galstyan, V., Bhandari, M. P., Sberveglieri, V., Sberveglieri, G., & Comini, E. (**2018). Metal oxide nanostructures in food applications: Quality control and packaging. Chemosensors, 6(2), 1–21.

[12] **Saengsrichan, A., Saikate, C., Silasana, P., Khemthong, P., Wanmolee, W., Phanthasri, J., Youngjan, S., et al.** (2022). The Role of N and S Doping on Photoluminescent Characteristics of Carbon Dots from Palm Bunches for Fluorimetric Sensing of Fe3+ Ion. International Journal of Molecular Sciences, 23(9). https://doi.org/10.3390/ijms23095001

[13] **Kalkan, Ö., Şahin, E., & Büyüktuncel, E.** (2017). Determination of Organic Acids in Natural and Commercial Orange Juices by HPLC/DAD. Hacettepe Journal of Biology and Chemistry, 3(45), 411–416.

[14] **Pajewska-Szmyt, M., Buszewski, B., & Gadzała-Kopciuch, R.** (2020). Sulphur and nitrogen doped carbon dots synthesis by microwave assisted method as quantitative analytical nano-tool for mercury ion sensing. Materials Chemistry and Physics, 242(November 2019).

[15] **Motaung, M. P., Onwudiwe, D. C., & Lei, W. (2021).** Microwave-Assisted Synthesis of Bi2S3and Sb2S3Nanoparticles and Their Photoelectrochemical Properties. ACS Omega, 6(29), 18975–18987.

[16] **Manzoor, S., Dar, A. H., Dash, K. K., Pandey, V. K., Srivastava, S., Bashir, I., & Khan, S. A.** (2023). Carbon dots applications for development of sustainable technologies for food safety: A comprehensive review. Applied Food Research, 3(1), 100263. https://doi.org/10.1016/ j.afres. 2023.100263

[17] **Basu, B., & Mehta, G. K.** (2014). Carbon nanotubes: A promising tool in drug delivery. International Journal of Pharma and Bio Sciences, 5(1).

[18] **Qi, B. P., Bao, L., Zhang, Z. L., & Pang, D. W. (2016**). Electrochemical Methods to Study Photoluminescent Carbon Nanodots: Preparation, Photoluminescence Mechanism and Sensing. ACS Applied Materials and Interfaces, 8(42), 28372–28382.

[19] **URL-1** <https://www.chemeurope.com>,en/encyclopedia/Hydrothermal_synthesis.html#:~:text=Hydrothermal%20synthesis%20can%20be%20defined,hot%20water%20under%20high%20pressure.

[20] **Stefanakis, D., Philippidis, A., Sygellou, L., Filippidis, G., Ghanotakis, D., & Anglos, D.** (2014). Synthesis of fluorescent carbon dots by a microwave heating process: structural characterization and cell imaging applications. Journal of Nanoparticle Research, 16(10). https://doi.org/10.1007/s11051-014-2646-1

[21] **Gao, S., Yan, S., Zhao, H., & Nathan, A.** (2021). Emerging Applications. Touch-Based Human-Machine Interaction, 179–229.

[22] **Li, L., Yu, B., & You, T. (2015).** Nitrogen and sulfur co-doped carbon dots for highly selective and sensitive detection of Hg (II) ions. Biosensors and Bioelectronics, 74, 263–269.

[23] **Kamali, S. R., Chen, C. N., Agrawal, D. C., & Wei, T. H.** (2021). Sulfur-doped carbon dots synthesis under microwave irradiation as turn-off fluorescent sensor for Cr(III). Journal of Analytical Science and Technology, 12(1).

[24] **Makalesi, A., Kübra Başkaya, S., & Çeşme, M.** (2021). Synthesis of N-Doped Carbon Quantum Dots by Hydrothermal Synthesis Method and Investigation of Optical Properties Hidrotermal Sentez Yöntemi ile N-Katkılı Karbon Kuantum Noktaları Sentezi ve Optik Özelliklerinin Araştırılması. Cilt, 10(2), 206–211.

[25] **Torvik, J. T.** (2000). Dopants in GaN. III-Nitride Semiconductors: Electrical, Structural and Defects Properties, 17–49.

[26] **Ali, A., Chiang, Y. W., & Santos, R. M.** (2022). X-Ray Diffraction Techniques for Mineral Characterization: A Review for Engineers of the Fundamentals, Applications, and Research Directions. Minerals, 12(2).

[27] **URL-2** <https://www.mt.com>,de/en/home/applications/L1_AutoChem_ Applications/Raman-Spectroscopy.html

[28] **Haiwen Ge, , Zhipeng Ye , Rui He.** (2005). Raman Spectroscopy of Diesel and Gasoline Engine-Out Soot Using Different Laser Power.

[29] **URL-3** <https://www.britannica.com>,science/filtration-chemistry

[30] **Srivastava, N., Singh, A., Kumari, P., Nishad, J. H., Gautam, V. S., Yadav, M., Bharti, R., Kumar, D., & Kharwar, R. N.** (2021). Advances in extraction technologies: isolation and purification of bioactive compounds from biological materials. In Natural Bioactive Compounds. Elsevier Inc.

[31] **Trevorah, R. M., Chantler, C. T., & Schalken, M. J.** (2019). Solving self-absorption in fluorescence. IUCrJ, 6, 586–602.

[32] **URL-4** <https://energyeducation.ca> ,encyclopedia/Band_gap

[33] **Moshinsky, M.** (1959). No Titleيليب. Nucl. Phys., 13(1), 104–116.

[34] **URL-5** <https://www.thermofisher.com>, tr/en/home/life-science/cell-analysis/cell-analysis-learning-center/molecular-probes-school-of-fluorescence/fluorescence-basics/anatomy-fluorescence-spectra.html

[35] **Lesani, P., Lu, Z., Singh, G., Mursi, M., Mirkhalaf, M., New, E. J., & Zreiqat, H.** (2021). Influence of carbon dot synthetic parameters on photophysical and biological properties. Nanoscale, 13(25), 11138–11149.

[36] **Bitterli, R., Kim, M., Scharf, T., Herzig, H.-P., Bich, A., Dumouchel, C., Roth, S., et al.** (2008). Refractive statistical concave 1D diffusers for laser beam shaping. Laser Beam Shaping IX, 7062(August), 70620P. https://doi.org/10.1117/12.793605

[37] **Lin, H., Huang, J., & Ding, L.** (2019). Preparation of Carbon Dots with High-Fluorescence Quantum Yield and Their Application in Dopamine Fluorescence Probe and Cellular Imaging. Journal of Nanomaterials, 2019.

[38] **Huang, H., Lv, J., Zhou, D., Bao, N., Xu, Y., & Wang, A.** (2013). RSC Advances. 21691–21696.

[39] **Hoan, B. T., Tam, P. D., & Pham, V.** (2019). Green Synthesis of Highly Luminescent Carbon Quantum Dots from Lemon Juice. 2019.

[40] **Microwave-Based Synthesis of Carbon Dots From Lemon Juice For Biotechnological Applications.** (2022). 5(2), 600–611.

[41] **Wang, S., Huo, X., Zhao, H., Dong, Y., Cheng, Q., & Li, Y.** (2022). One-pot green synthesis of N , S co-doped biomass carbon dots from natural grapefruit juice for selective sensing of Cr (VI). 5(October).

[42] **Links, D. A.** (2012). ChemComm Simple one-step synthesis of highly luminescent carbon dots from orange juice : application as excellent bio-imaging agents w. 8835–8837.

[43] **Lai, Z., Guo, X., Cheng, Z., Ruan, G., & Du, F.** (2020). Green Synthesis of Fluorescent Carbon Dots from Cherry Tomatoes for Highly Effective Detection of Trifluralin Herbicide in Soil Samples. ChemistrySelect, 5(6), 1956–1960.

[44] **Zhang, D., Zhang, F., Liao, Y., Wang, F., & Liu, H.** (2022). Carbon Quantum Dots from Pomelo Peel as Fluorescence Probes for "Turn-Off–On" High-Sensitivity Detection of Fe3+ and L-Cysteine. Molecules, 27(13).

[45] **Surendran, P., Lakshmanan, A., Priya, S. S., Geetha, P., Rameshkumar, P., Kannan, K., Hegde, T. A., et al.** (2021). Fluorescent carbon quantum dots from Ananas comosus waste peels: A promising material for NLO behaviour, antibacterial, and antioxidant activities. Inorganic Chemistry Communications, 124(November 2020), 108397. https://doi.org/10.1016/j.inoche.2020.108397

[46] **Ludmerczki, R., Mura, S., Carbonaro, C. M., Mandity, I. M., Carraro, M., Senes, N., Garroni, S., et al.** (2019). Carbon Dots from Citric Acid and its Intermediates Formed by Thermal Decomposition. Chemistry - A European Journal, 25(51), 11963–11974. https://doi.org/10.1002/chem.201902497

[47] **Mohammad-Jafarieh, P., Akbarzadeh, A., Salamat-Ahangari, R., Pourhassan-Moghaddam, M., & Jamshidi-Ghaleh, K.** (2021). Solvent effect on the absorption and emission spectra of carbon dots: evaluation of ground and excited state dipole moment. BMC Chemistry, 15(1), 1–10.

[48] **V, L., P, P., & A, V.** (2017). Effect of solvent polarity on fluoroscence spectra of camphor Sulphonic acid doped Polyaniline. Madridge Journal of Analytical Sciences and Instrumentation, 2(1), 21–24.

[49] **URL-6** <https://www.chem.rochester.edu>,/notvoodoo/pages/reagents.php?page=solvent_polarity

[50] **URL-7** <https://people.chem.umass.edu>,xray/solvent.html

[51] **Jorge, M., Gomes, J. R. B., & Barrera, M. C.** (2022). The dipole moment of alcohols in the liquid phase and in solution. Journal of Molecular Liquids, 356, 119033.

[52] **Yoshinaga, T., Shinoda, M., Iso, Y., Isobe, T., Ogura, A., & Takao, K. I.** (2021). Glycothermally Synthesized Carbon Dots with Narrow-Bandwidth and Color-Tunable Solvatochromic Fluorescence for Wide-Color-Gamut Displays. ACS Omega, 6(2),

[53] **Popczyk, A., Cheret, Y., El-Ghayoury, A., Sahraoui, B., & Mysliwiec, J.** (2020). Solvatochromic fluorophores based on thiophene derivatives for highly-precise water, alcohols and dangerous ions detection. Dyes and Pigments, 177(January).

[54] **Pramanik, A., Biswas, S., & Kumbhakar, P.** (2018). Solvatochromism in highly luminescent environmental friendly carbon quantum dots for sensing applications: Conversion of bio-waste into bio-asset. Spectrochimica Acta - Part A: Molecular and Biomolecular Spectroscopy, 191, 498–512.

[55] **Shaikh, A. F., Tamboli, M. S., Patil, R. H., Bhan, A., Ambekar, J. D., & Kale, B. B.** (2018). Bioinspired Carbon Quantum Dots: An Antibiofilm Agents. Journal of Nanoscience and Nanotechnology, 19(4), 2339–2345.

[56] **Das, P., Ganguly, S., Maity, P. P., Srivastava, H. K., Bose, M., Dhara, S., Bandyopadhyay, S., et al.** (2019). Converting waste Allium sativum peel to nitrogen and sulphur co-doped photoluminescence carbon dots for solar conversion, cell labeling, and photobleaching diligences: A path from discarded waste to value-added products. Journal of Photochemistry and Photobiology B: Biology, 197(December 2018), 111545. https://doi.org/10.1016/j.jphotobiol.2019.111545

[57] **URL-8** <https://www.sigmaaldrich.com>,TR/en/technical-documents/technical-article/analytical-chemistry/photometry-and-reflectometry/ir-spectrum-table

[58] **Information, S. (n.d.).** Glycothermally Synthesized Carbon Dots with Solvatochromic Fluorescence for Wide-Color-Gamut. 1558, 3–14.

[59] **Sun, C., Zhang, Y., Wang, P., Yang, Y., Wang, Y., Xu, J., Wang, Y., et al.** (2016). Synthesis of Nitrogen and Sulfur Co-doped Carbon Dots from Garlic for Selective Detection of Fe 3 +. Nanoscale Research Letters. https://doi.org/10.1186/s11671-016-1326-8

[60] **Konwar, A., Gogoi, N., Majumdar, G., & Chowdhury, D.** (2015). Green chitosan-carbon dots nanocomposite hydrogel film with superior properties. Carbohydrate Polymers, 115, 238–245.

CURRICULUM VITAE

Name Surname **:** Anita NABII

EDUCATION :

- **B.Sc.** **:** 2018, Islamic Azad University of Tabriz, Iran. Faculty of Electric Electeronic, Department of Bio-medical Engineering

CONFERENCE :

- **Anita Nabii**, Ferhat Erden, Hilmi Ünlü, Mesut Balaban. (2022). Colloidal Synthesis and Characterization of Carbon Quantum Dots, 16th Nano science and nanotechnology conference (Nano-TR 16), Ankara-Turkey (Poster presentation)